E：膨潤土內的化學交換行為(Alteration behavior)

E.1：Abstract－Effect of initial dry density of compacted bentonite on interaction with cementitious material

Title:

Effect of initial dry density of compacted bentonite on interaction with cementitious material

Abstract:

An engineered barrier of the radioactive waste disposal facility has been required to have suitable physicochemical properties and long-term stability. Bentonite and cementitious materials that have the potential to be used in engineered barriers for the radioactive waste disposal facility would be gradually altered by reactions with groundwater. Therefore, it is necessary to understand the alteration and interaction behaviors of these promising engineered barriers for assessing the long-term safety of the radioactive waste disposal. Our major goals in this study were (1) to understand the interaction behavior between the compacted bentonite and the cementitious material and (2) to evaluate the effect of the initial dry density of the compacted bentonite on the interaction behavior.

The contacted specimens of the hardened cementitious material (OPC) with the compacted bentonites were immersed in deionized water at 20°C for 2.5 years. In the experiments, the hardened OPC with a water/cement ratio of 40% and compacted bentonites (Kunigel V1) with different initial dry densities (1.0, 1.2, 1.4 and 1.6 Mg/m^3) were used. The immersion fluid (deionized water) was exchanged with fresh deionized water at intervals of about one month. The pH of the immersion fluids was obtained using a pH meter. The mineralogy and the chemical compositions of the contacted specimens were analyzed by XRD and EPMA, respectively.

The pH of each immersion fluid was constant (about 10.4) during the experiments, which was independent of the initial dry density of the compacted bentonites. The present pH value is lower than that of the previous study in which the leaching experiment was carried out on a single piece of hardened OPC paste (about pH=11.4) [1].

The leaching rates of cement hydrates (i.e., Portlandite and calcium silicate hydrate) in the hardened OPC of the contacted specimens, which were estimated from Ca content, did not increase as rapidly as those in the previous study[1]. The degree of leaching of cement hydrates was inhibited with the increase of initial dry density of the compacted bentonite.

No changes were observed in the mineral compositions of the

compacted bentonites, but the ratio of Ca/Na in the compacted bentonite was dependent on its initial dry density. The Ca/Na value of 1.0 Mg/m^3 was greater than that of 1.6 Mg/m^3. These results showed that Na in montmorillonite of the compacted bentonite was exchanged with Ca which was generated by the leaching of the cement hydrate, and its exchange degree decreased with the increase of the initial dry density.

In conclusion, the leaching of the cement hydrates should be inhibited by the contact with the compacted bentonite with a high dry density. Moreover, Ca-exchange reaction of Na-montmorillonite is controlled by this inhibition of Ca generation by leaching of the cement hydrates.

1) Hironaga, H. and Yamamoto, T. (2005) Civil Engineering Research Laboratory Rep. N04027 in Japanese with English abstract.

E.2：Slides－Effect of initial dry density of compacted bentonite on interaction with cementitious material

Effect of initial dry density of compacted bentonite on interaction with cementitious material

Shingo YOKOYAMA and Michihiko HIRONAGA
[CRIEPI]

PURPOSE

To understand the interaction behavior between the compacted bentonite and the cementitious materials.

To estimate the effect of the initial dry density of the compacted bentonite on the interaction behavior.

SAMPLE

Compacted Bentonite

Bentonite: Kunigel V1 (Yamagata prefecture, Japan)
Mineral composion: Montmorillonite, Quartz, Feldspar, Calcite, Dolomite, Pyrite, Clinoptilolite
Initial dry density: 1.0, 1.2, 1.4, 1.6 Mg/m^3
Diameter and height: 20 mm, 20 mm

Cementitious Material

Cement: ordinary Portland cement (OPC)
Water/Cement mass ratio: 0.4
Diameter and height: 17.65 mm, 20 mm
Curing Temperature: 50 °C
Curing Time: 3 month

METHOD

Immersing of experimental holder in deionized water

↓

Vacuum for about 12 hours

↓

Keep in a N_2 filled glove box for 4 or 5 weeks at 20 °C

The immersing solution has to be exchanged the fresh deionized water

No ← Has the immersing solution been exchanged for fresh deionized water 30 times?

Yes ↓

Analysis of the contacted specimens (XRD and EPMA)

Immersion experiment

Solution: Deionized waster (244.5g)

Temperature: 20 °C

Condition: Nitrogen filled glove box

Total immersing time: 130 weeks (2.5 y)

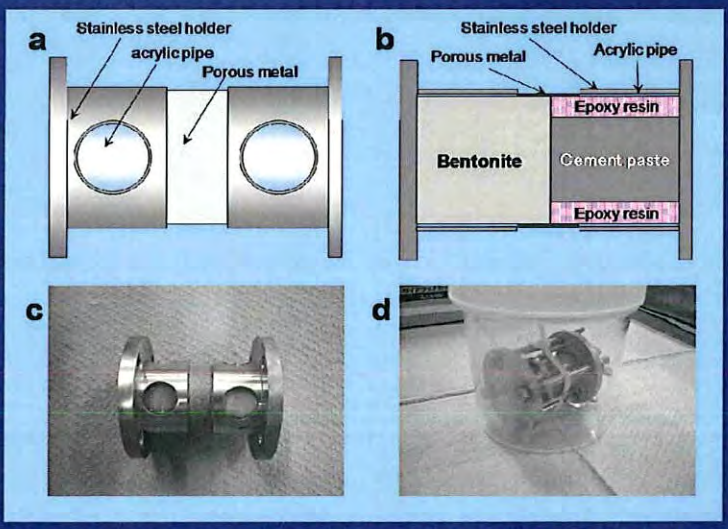

Schematic diagrams and photos of the experimental stainless steel holder containing the contacted specimens.

RESULTS: XRD ; CEMENT PASTE

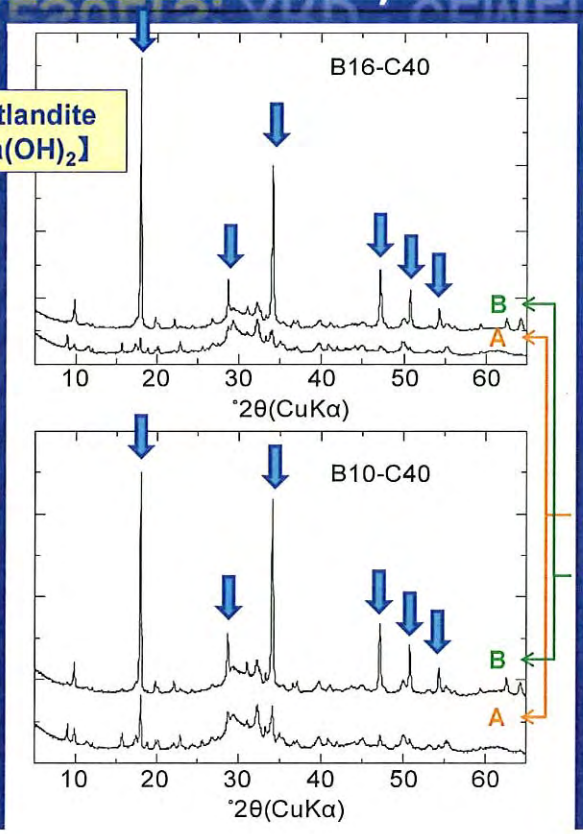

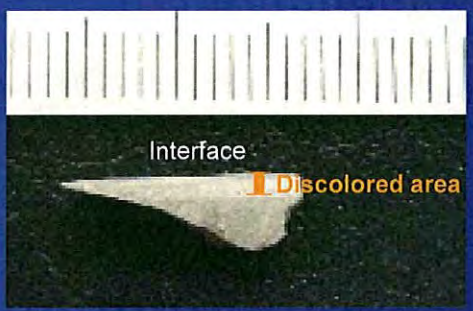

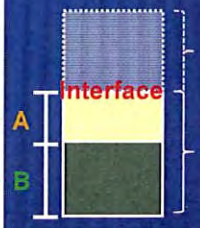

Compacted bentonite

Cementitious material

	B10-C40	B12-C40	B14-C40	B16-C40
A	1.7 mm	1.8 mm	1.3 mm	1.2 mm

RESULTS: XRD ; CEMENT PASTE

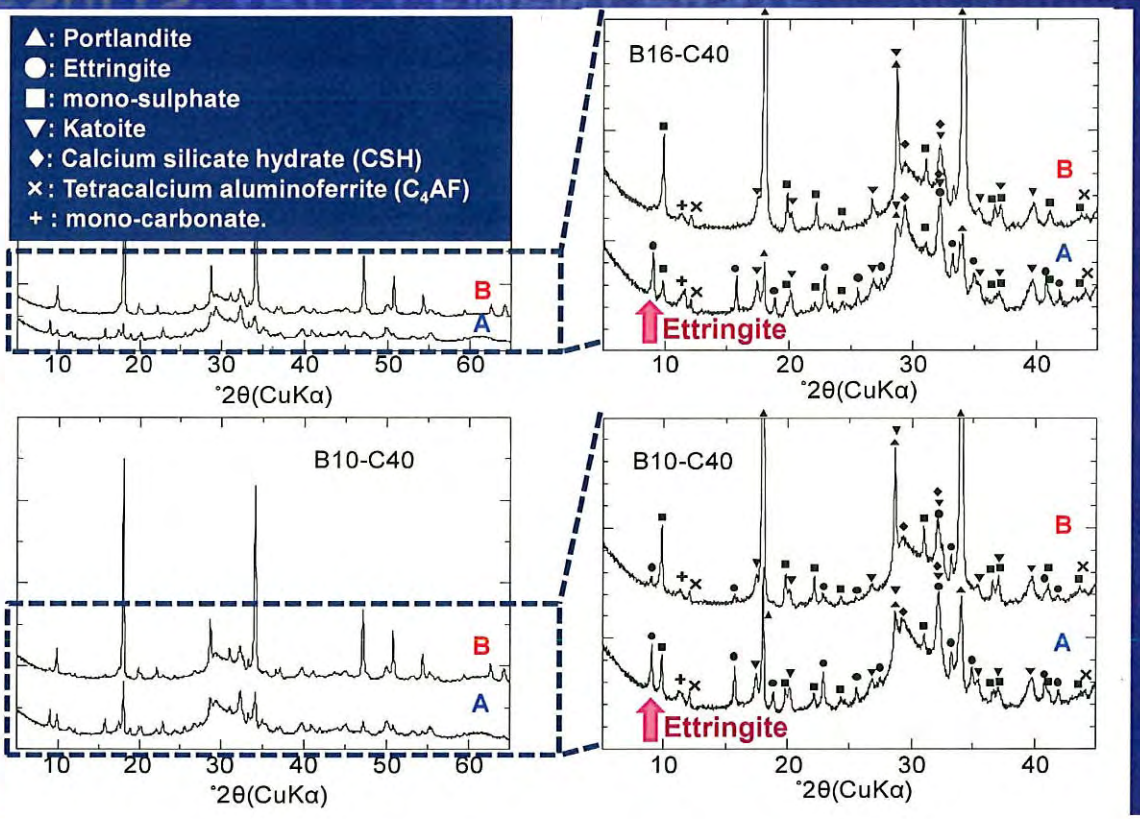

RESULTS: EPMA ; CEMENT PASTE

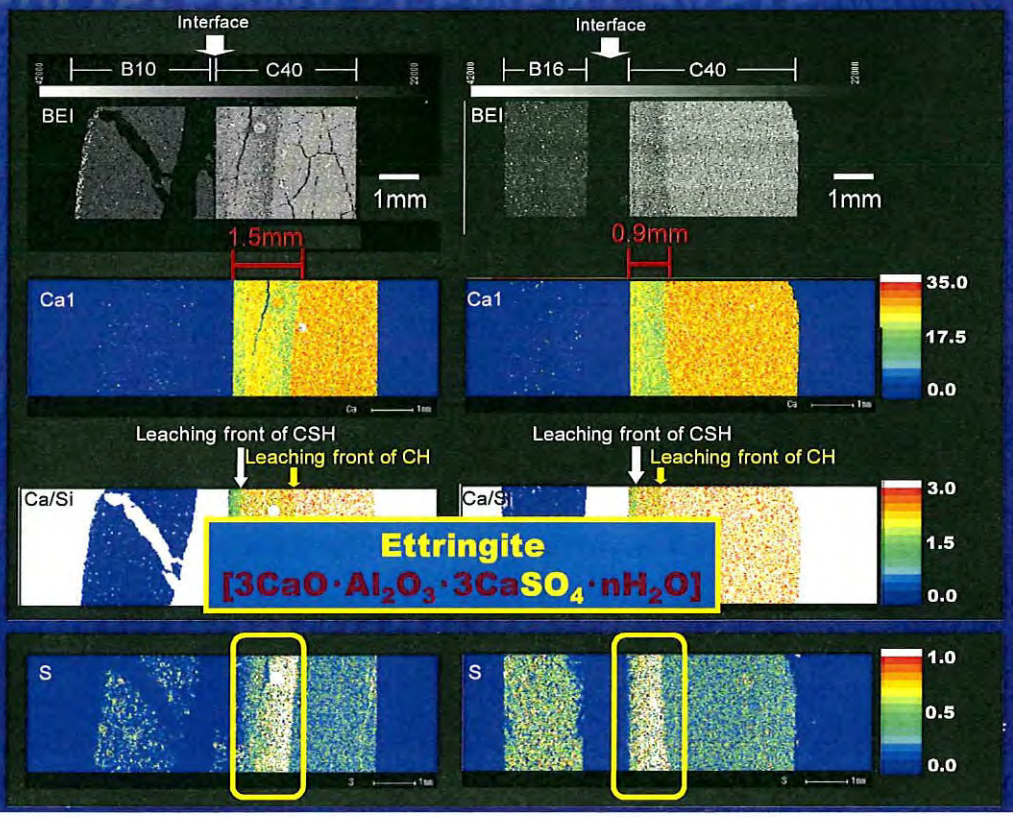

RESULTS: XRD ; COMPACTED BENTONITE

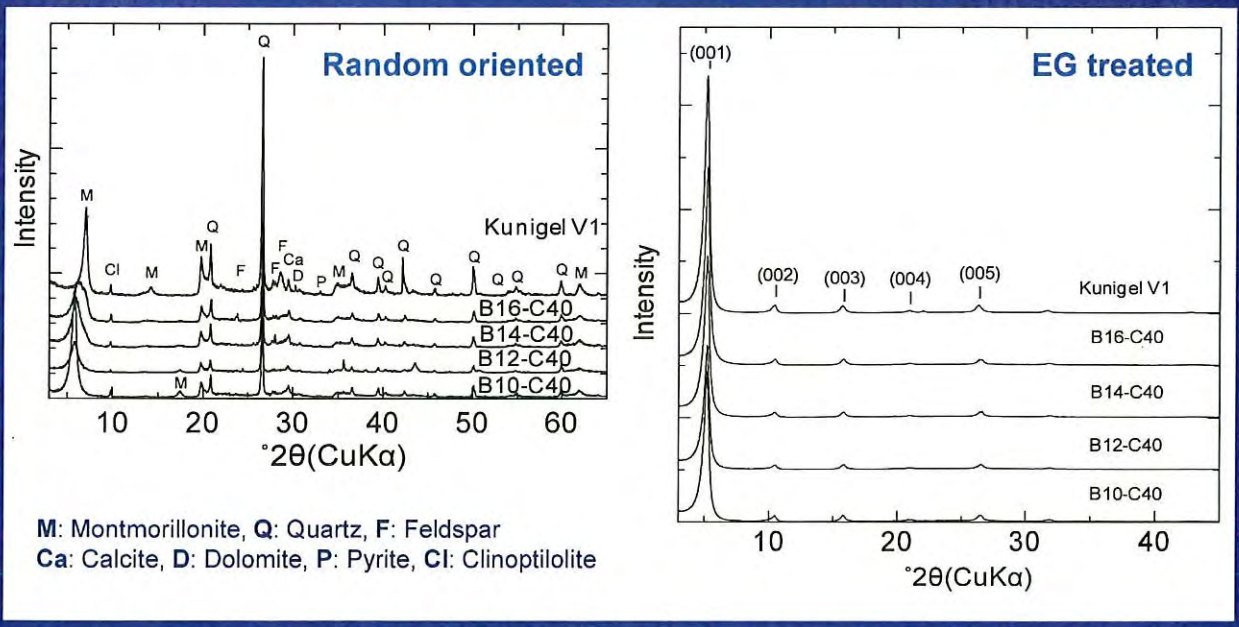

M: Montmorillonite, **Q**: Quartz, **F**: Feldspar
Ca: Calcite, **D**: Dolomite, **P**: Pyrite, **Cl**: Clinoptilolite

- No changes of the mineral compositions of the compacted bentonite were observed.
- No changes of the mineralogical natures of the montmorillonite were observed.

RESULTS: EPMA ; COMPACTED BENTONITE

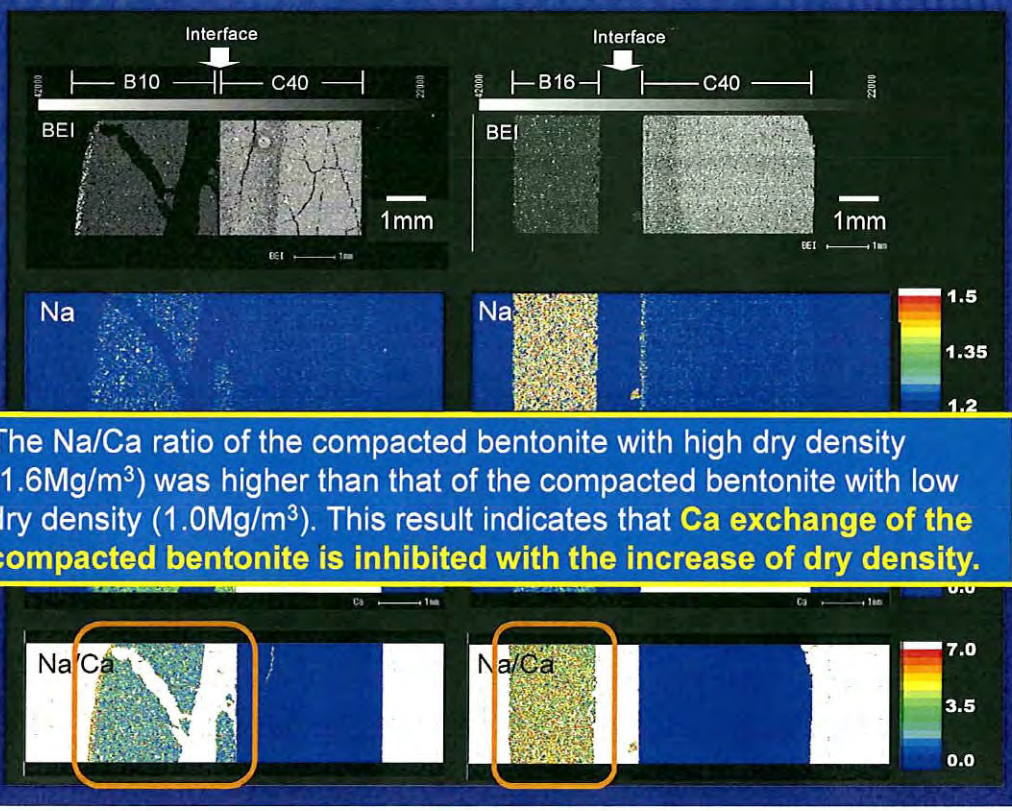

The Na/Ca ratio of the compacted bentonite with high dry density (1.6Mg/m^3) was higher than that of the compacted bentonite with low dry density (1.0Mg/m^3). This result indicates that **Ca exchange of the compacted bentonite is inhibited with the increase of dry density.**

CONCLUSION

- Leaching of the cement hydrate was inhibited due to the fact that cementitious materials are contacted with the compacted bentonite. Furthermore, a degree of inhibition was increased with the dry density of the compacted bentonite.
- Ettringite as a secondary mineral was precipitated in the leaching area of portlandite.
- No change of the mineral components of the compacted bentonite were observed.
- Ca exchange of the compacted bentonite which is caused by Ca leaching from cement paste was inhibited with the increase of the dry density of the compacted bentonite.

The leaching of the cementitious material should be inhibited by the contact with the high-dry density compacted bentonite. Consequently, Ca-exchange reaction with montmorillonite is controlled by this inhibition of Ca generation by leaching of the cement hydrates.

E.3：Poster－Effect of initial dry density of compacted bentonite on interaction with cementitious material

EFFECT OF INITIAL DRY DENSITY OF COMPACTED BENTONITE ON INTERACTION WITH CEMENTITIOUS MATERIAL

Shingo YOKOYAMA and Michihiko HIRONAGA
(Central Research Institute of Electric Power Industry)

INTRODUCTION:

An engineered barrier of the radioactive waste disposal facility has been required to have suitable physicochemical properties and long-term stability. Bentonite and cementitious materials that have the potential to be used in engineered barriers for the radioactive waste disposal facility would be gradually altered by reactions with groundwater. Therefore, it is necessary to understand the alteration and interaction behaviors of these promising engineered barriers for assessing the long-term safety of the radioactive waste disposal. Our major goals in this study were (1) to understand the interaction behavior between the compacted bentonite and the cementitious material and (2) to evaluate the effect of the initial dry density of the compacted bentonite on the interaction behavior.

SAMPLES AND METHODS:

Compacted Bentonite

Bentonite: Kunigel V1
Mineral component: Montmorillonite, Quartz, Feldspar, Calcite, Dolomite, Pyrite, Clinoptilolite
Initial dry density: 1.0, 1.2, 1.4, 1.6 Mg/m^3
Diameter and height: 20 mm, 20 mm

Cementitious Material

Cement: ordinary Portland cement (OPC)
Water/Cement mass ratio: 0.4
Diameter and height: 17.65 mm, 20 mm
Curing Temperature: 50 ºC
Curing Time: 3 month

Immersion Experiment

Solution: Deionized waster (244.5g)
Temperature: 20 ºC
Condition: Nitrogen filled glove box
Total immersing time: 130 weeks (2.5 y)

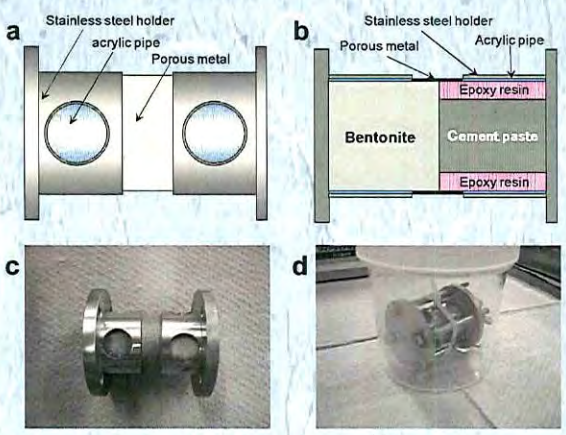

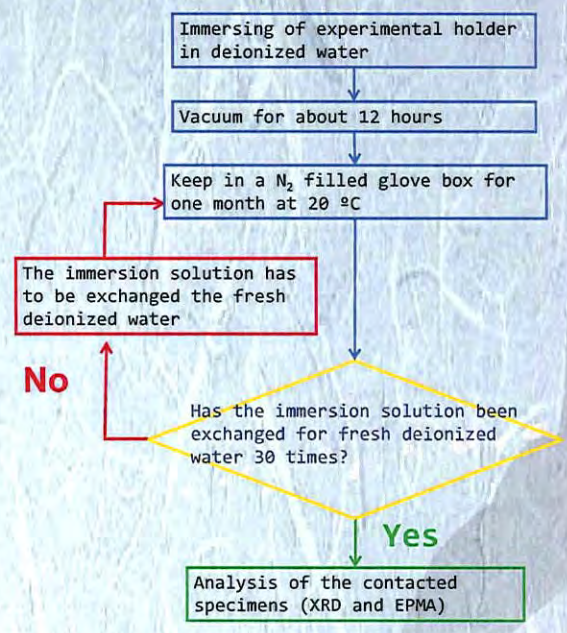

RESULTS AND DISCUSSION:

Immersion Solutions

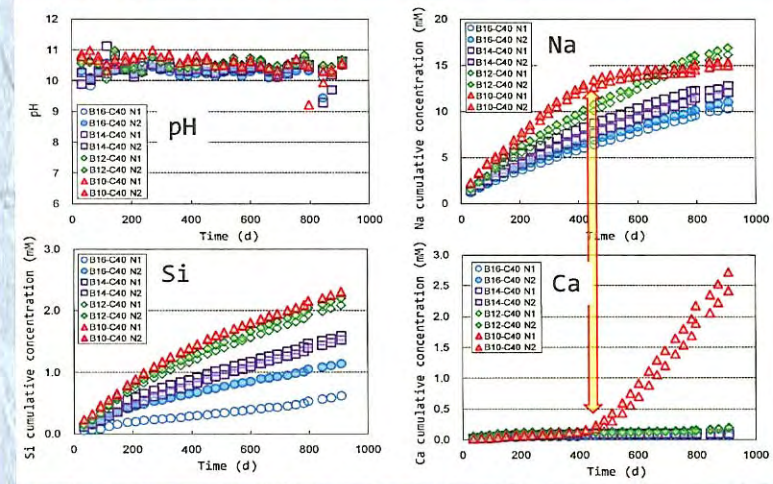

Fig. Solution Chemistry of Immersion Solutions.

The pH of each immersion solution was constant (about 10.4) during the experiments, which was independent of the initial dry density of the compacted bentonites. Si cumulative concentration increased with time. And Si cumulative concentration increased with decrease the initial dry density.

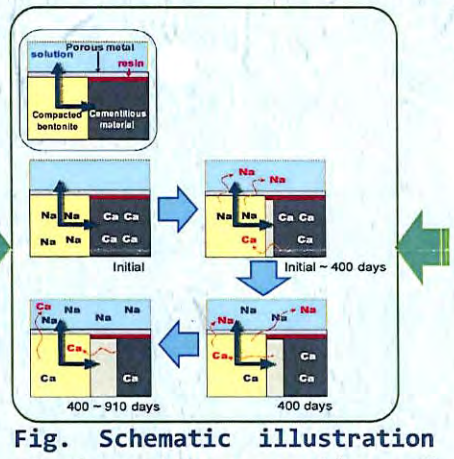

Fig. Schematic illustration of Ca-exchange reaction of compacted bentonite with dry density of 1.0 Mg/m^3.

Compacted Bentonites

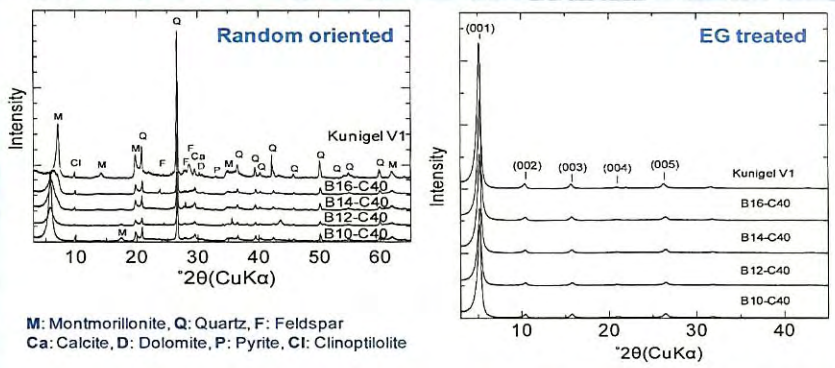

M: Montmorillonite, Q: Quartz, F: Feldspar
Ca: Calcite, D: Dolomite, P: Pyrite, Cl: Clinoptilolite

Fig. XRD patterns of compacted bentonites.

Mineral compositions of the compacted bentonites after immersion experiments were the same as the original Kunigel V1 (left Fig.). Changes of the mineralogical natures of the montmorillonite, i.e. illitization, didn't occur (right Fig.).

Cement Pastes

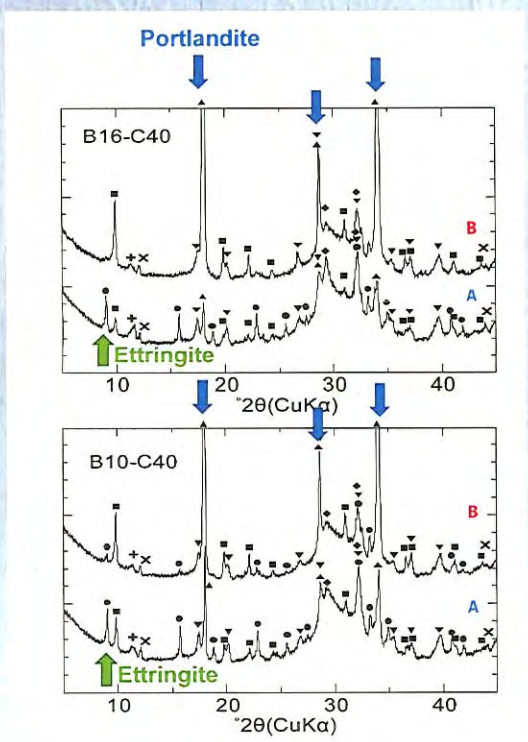

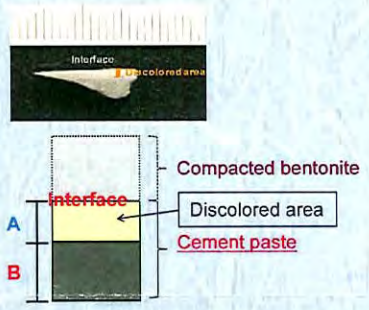

In each cement paste of contacted specimen, discolored area was observed around the interface. In the sample collected discolored area, the peaks intensities of Portlandite were weak in compare with non-discolored area. This result indicate that Portlandite was dissolved in discolored area. On the other hand, new peak of Ettringite, which is secondary mineral was observed in the sample collected discolored area.

Fig. XRD patterns of cement paste.

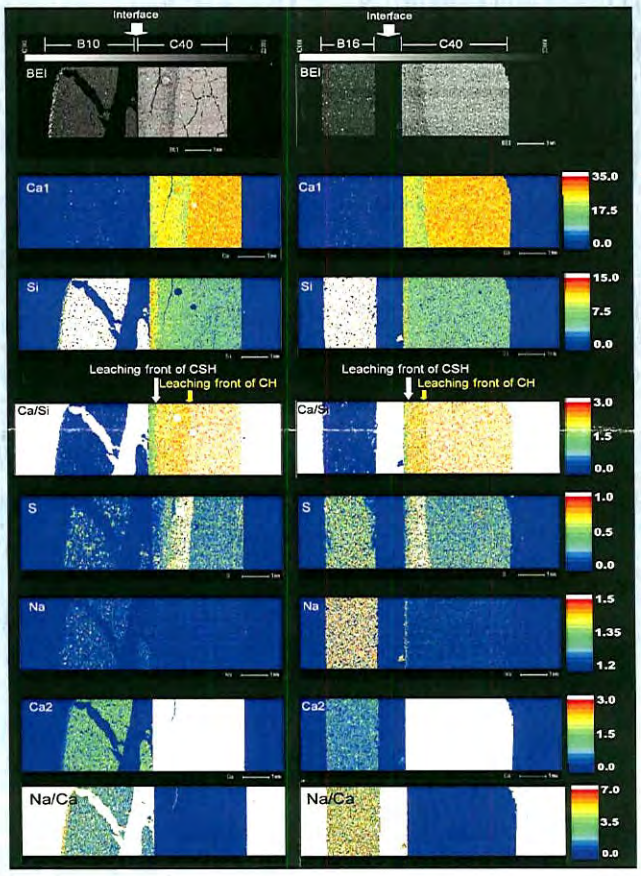

In the previous leaching experiment of a single piece of hardened OPC under the similar experiment condition, the leaching front of Portlandite reached to a depth of 1.5 mm from surface in only 23 weeks. In this study, since the leaching fronts of Portlandite were less than 1.5mm in 130 weeks, the leaching of cement hydrate, as Portlandite, was inhibited due to the fact that the cementitious material are contacted with compacted bentonite. The leaching of cement hydrates as Portlandite and CSH inhibited with the increase of initial dry density of the compacted bentonite.

High concentration of sulfur was observed in leaching part of Portlandite. It is caused by the precipitation of Ettringite as secondary mineral.

The ratio of Na/Ca in the compacted bentonite was dependent on its initial dry density. The Na/Ca value of initial dry density of 1.6 was greater than that of 1.0. This result indicates that Ca exchange reaction of the montmorillonite in the compacted bentonite is inhibited with the increase of initial dry density.

Fig. EPMA images of B10-C40 (left) and B16-C40 (right).

CONCLUTION:

The leaching of the cement hydrates should be inhibited by the contact with the compacted bentonite with a high dry density.
Moreover, Ca-exchange reaction of Na-montmorillonite is controlled by this inhibition of Ca generation by leaching of the cement hydrates.

F：膨潤土膨脹行為

F.0：Slides－Summary of Training by Yukihisa Tanaka

Summary of Training by Yukihisa Tanaka

November 14, 2012

Central Research Institute of Electric Power Industry
Yukihisa Tanaka

Items for training

1. Modeling hydraulic conductivity and swelling pressure of compacted bentonite affected by salinity of water

2. Swelling model for compacted bentonite during infiltration of water

3. Gas migration characteristics of compacted bentonite

Modeling Hydraulic Conductivity and Swelling Pressure of Compacted Bentonite Affected by Salinity of Water

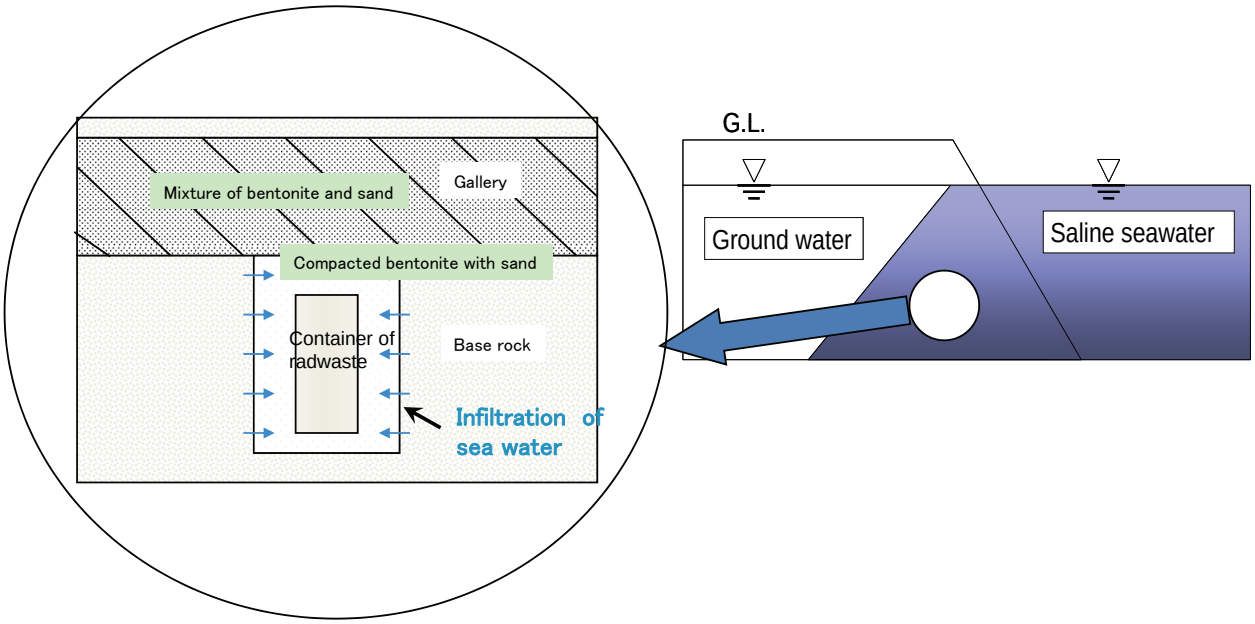

Modeling Hydraulic Conductivity and Swelling Pressure of Compacted Bentonite Affected by Salinity of Water

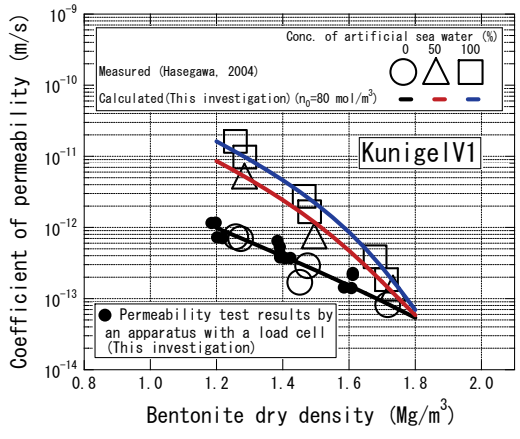

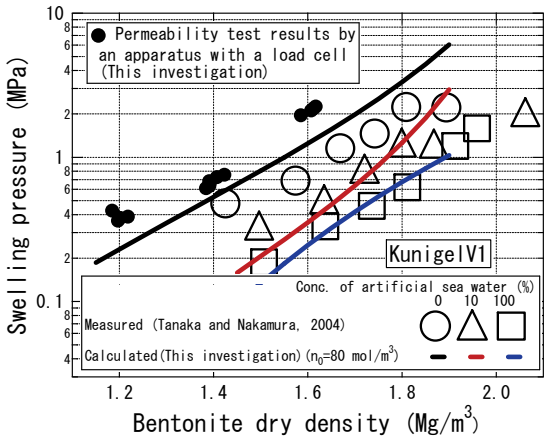

・In this research, a new stress-strain model of compacted bentonite is proposed.
・By this model , the effect of salinity of water can be evaluated.
・As shown in these figures, test results coincide well with calculated results by the proposed model.

Proposal of Dual Swelling Mechanism Model for Saturated and Unsaturated Compacted Bentonite

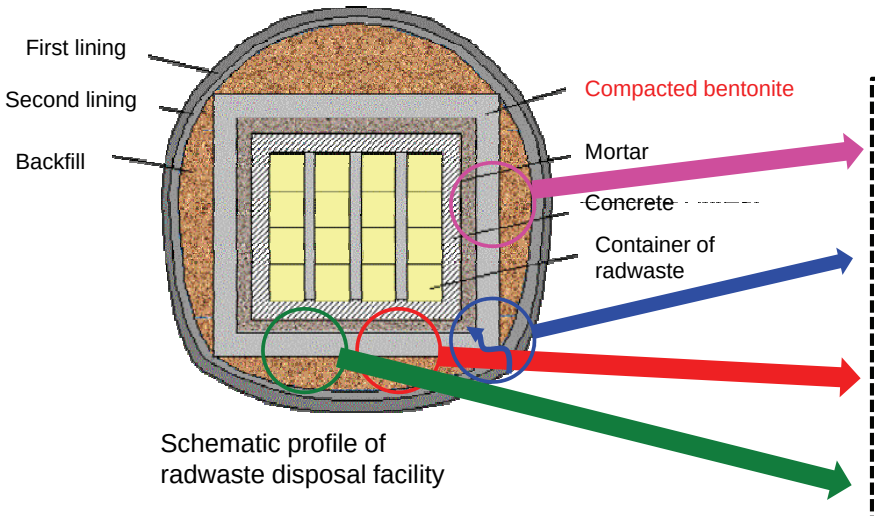

Schematic profile of radwaste disposal facility

Expected events during infiltration of water

- Mechanical interaction between compacted bentonite and base rock.
- Displacement of radwaste container by ununiform infiltration of groundwater.
- Redistribution dry density caused by swelling pressure.
- Settlement of radwaste container due to softening of base bentonite.

Swelling model of compacted bentonite during infiltration of water is necessary.

Proposal of Dual Swelling Mechanism Model for Saturated and Unsaturated Compacted Bentonite

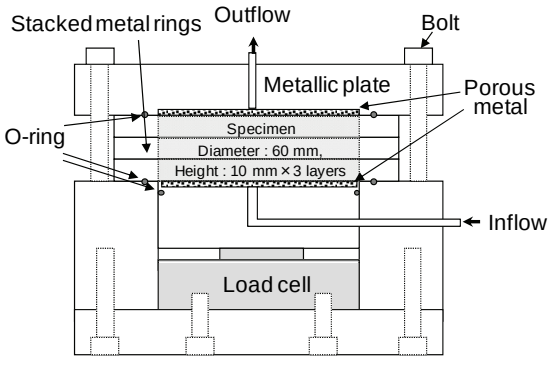

(a) Test apparatus

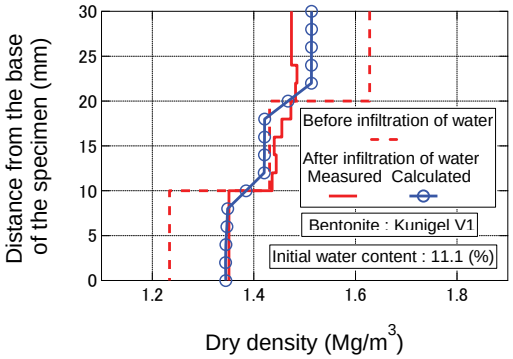

(b) Test results and calculated results

・In this research, swelling model of compacted bentonite during infiltration of water is proposed.
・This model can express swelling by osmotic pressure as well as reduction of suction.
・As shown in this figure, redistribution of dry density of compacted bentonite can be simulated with accuracy.

Development of numerical Simulation Method for Gas Migration through Compacted Bentonite using Model of Two-Phase Flow through Deformable Porous Media

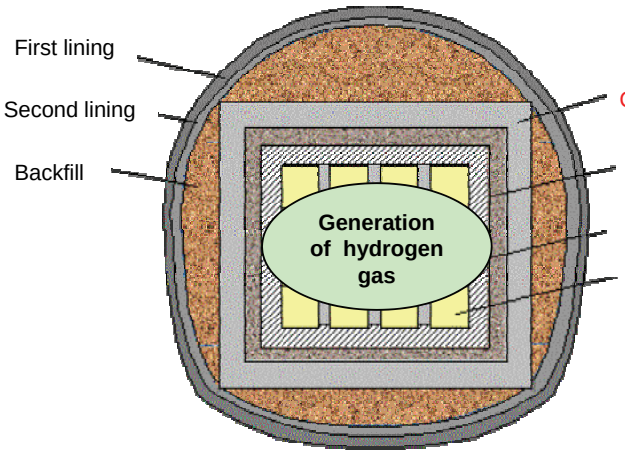

Schematic profile of radwaste disposal facility

Hydrogen gas will generate inside of the engineered barrier because of anaerobic corrosion of metal used for containers, etc.

Permeability of compacted bentonite is very small. Thus, it would be difficult for the generated gas to migrate through the compacted bentonite.

It is important to evaluate gas migration characteristics of compacted bentonite

Development of Numerical Simulation Method for Gas Migration through Compacted Bentonite using Model of Two-Phase Flow through Deformable Porous Media

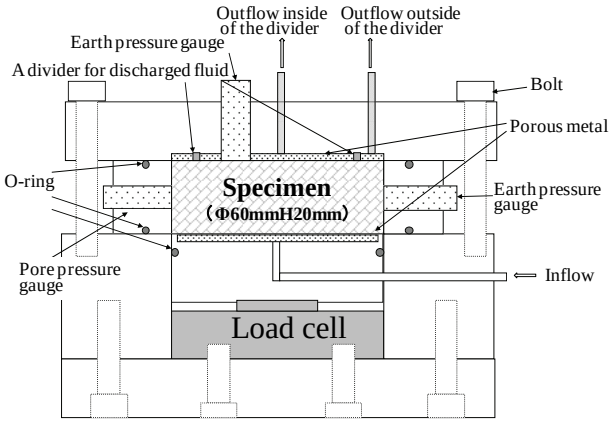

(a) Apparatus gas migration test

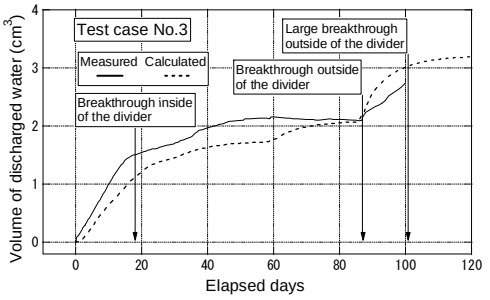

(b) Volume of discharged water

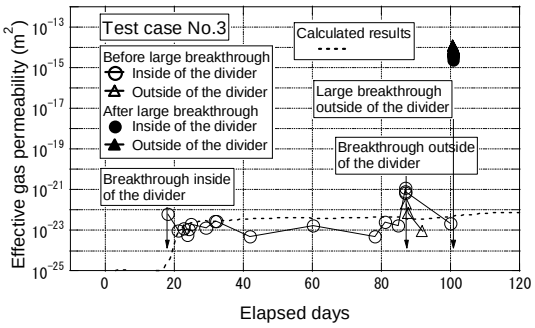

(c) Effective gas permeability

・In this research, numerical simulation method for gas migration through compacted bentonite is proposed.
・By this method, test results can be simulated with accuracy.

F.1：Abstract－Dual Swelling Mechanism Model for Saturated and Unsaturated Compacted Bentonite

An abstract for 5th International meeting "Clays in Natural and Engineering Barriers for Radioactive Waste Confinement" Montpellier – October 22-25, 201

Dual Swelling Mechanism Model for Saturated and Unsaturated Compacted Bentonite

Y. Tanaka[1]

1. Fuel Cycle Backend Research Center, Civil Engineering Research Laboratory, Central Research Institute of Electric Power Company, 1646 Abiko, Abiko-shi, Chiba-ken, Japan (yu-tanak@criepi.denken.or.jp)

In the current concept of repository for radioactive waste disposal, compacted bentonite as well as bentonite-based material will be used as an engineered barrier mainly for inhibiting migration of radioactive nuclides. Since compacted bentonite swells when it is saturated, dry density of compacted bentonite will be redistributed and container of radioactive wastes will move during infiltration of underground water. Accurate evaluation of these events is effective in decreasing uncertainty in long term safety evaluation of radioactive waste facilities. However, sufficient evaluation is not conducted because behaviour of bentonite material during saturation process is not clarified sufficiently. Thus, stress-strain model of bentonite material during saturation process is proposed and applicability of the model is investigated (Tanaka, 2012).

It is well known that compacted bentonite swells with large deformation by infiltration of water. Swelling behaviour of bentonite is mainly attributable to osmotic pressure caused by the difference between concentration of ions inside of montmorillonite flakes and that outside of montmorillonite flakes. Thus, swelling which is attributable to osmotic pressure is named "swelling by osmotic pressure" here. By contrast, unsaturated ordinary clay swells or shrinks during infiltration of water without effect of osmotic pressure. Since this phenomenon is mainly attributable to reduction of suction during infiltration of water, it is reasonable to assume that unsaturated bentonite swells or shrinks during infiltration of water by reduction of suction. Thus, swelling which is attributable to reduction of suction is named "swelling by reduction of suction" here. It is assumed in this paper that swelling by osmotic pressure occurs when bentonite is fully saturated, while swelling by reduction of suction occurs when bentonite is unsaturated.

Axial strain increment $d\varepsilon_a$ of a cylinder specimen due to swelling by reduction of suction is expressed by the following equation (Tanaka, 2012) :

$$d\varepsilon_a = d\sigma'_a / K_{d1} + \left(-dK_{d1}/K_{d1} \cdot \sigma'_m + \beta \cdot S_{w,e} \cdot du_c\right)/K_{d1} \quad (1)$$

where, K_{d1} : one dimensional bulk modulus, $S_{w,e}$: effective saturation of water, β : a parameter which is depending on dry density, u_c : suction, σ'_m : mean effective stress, $d\sigma'_a$: effective axial stress increment

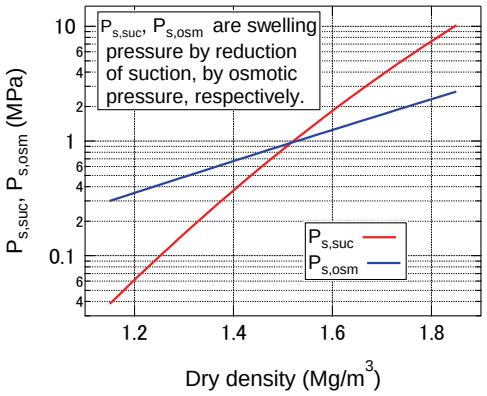

Figure 1 : Swelling pressure VS dry density

It should be noted that Eq.(1) can express not only swelling but also shrinkage because K_{d1} decreases during saturation process. Effective axial stress increment $d\sigma'_a$ can be calculated by assuming $d\varepsilon_a$=0 in Eq.(1). By integrating $d\sigma'_a$, swelling pressure by reduction of suction under integrity constraints, $P_{s,suc}$, can be calculated. $P_{s,suc}$ measured by experiments is plotted as a red solid line in Fig.1. Let $P_{s,suc}$ by calculation equal $P_{s,suc}$ by experiments, β in Eq.(1) is determined. By contrast, the relationship between $P_{s,osm}$ and dry density is also plotted as a blue solid line in Fig.1. Swelling pressure measured by swelling pressure test equals larger one of $P_{s,suc}$ and $P_{s,osm}$.

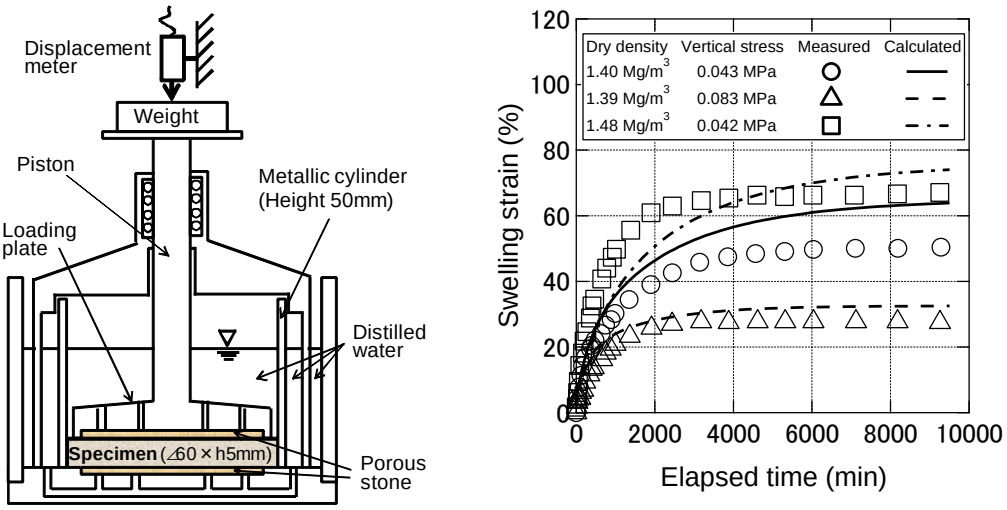

(a) Test apparatus (b) Test results and calcurated results

Figure 2 : Swelling deformation test under a constant vertical load

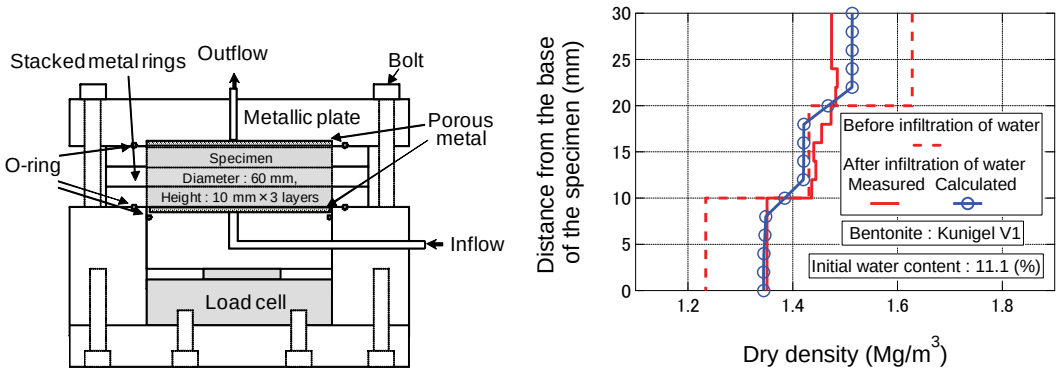

(a) Test apparatus (b) Test results and calcurated results

Figure 3 : Swelling test for a specimen with heterogeneous dry density

Swelling deformation under a constant vertical load is measured by the apparatus shown in Fig. 2(a). Axial strain during infiltration process is calculated by Eq. (1). Since constant axial stress P_v by weight, which is applied to the specimen throughout infiltration of water, is smaller than $P_{s,osm}$, excess pore water pressure of P_v - $P_{s,osm}$ generates immediately after fully saturation. Then axial strain generates by dissipation of the excess pore water pressure. As shown Fig. 2(b), the calculated results are accordant with the measured results.

Figure 3(a) shows a swelling test apparatus for a specimen with heterogeneous dry density (Tanaka, 2012). As shown in Fig. 3(b), dry density after infiltration of water is less heterogeneous than that before infiltration of water. Calculated results are also plotted in Fig.3(b). As shown Fig. 3(b), the calculated results are accordant with the measured results.

Reference:

Tanaka, Y. 2012. Modelling swelling process of compacted bentonite (Part 2), Proposal of swelling model for saturated and unsaturated bentonite and its verification, *Report of Central Research Institute of Electric Power Industry, N11035*, (in Japanese)

F.2：Poster－Dual Swelling Mechanism Model for Saturated and Unsaturated Compacted Bentonite

A poster which was presented in 5th International meeting “Clays in Natural and Engineering Barriers for Radioactive Waste Confinement, Montpellier – October 22-25, 2012

Dual Swelling Mechanism Model for Saturated and Unsaturated Compacted Bentonite

Central Research Institute of Electric Power Industry
Yukihisa Tanaka

Introduction : In the current concept of repository for radioactive waste disposal in Japan, compacted bentonite as well as bentonite-based material will be used as an engineered barrier mainly for inhibiting migration of radioactive nuclides. Since compacted bentonite swells when it is saturated, dry density of compacted bentonite will be redistributed and container of radioactive wastes will move during infiltration of underground water. Accurate evaluation of these events is effective in decreasing uncertainty in long term safety evaluation of radioactive waste facilities. However, sufficient evaluation is not conducted because behaviour of bentonite material during saturation process is not clarified sufficiently. Thus, stress-strain model of bentonite material during saturation process is proposed and applicability of the model is investigated.

Microstructure features and schematic picture of Na montmorillonite

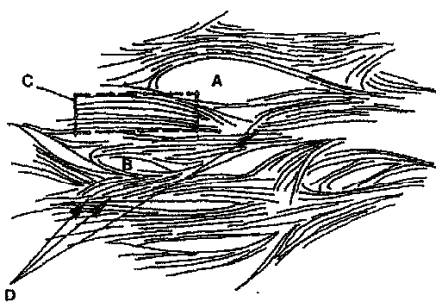

Fig.1 Microstructural features of smectite clay Na montmorillonite clay : A=large pore, B=small void with external water, C=stack or “quasicrystal” with organized water, D=interface between stacks (Pusch et al, 1990)

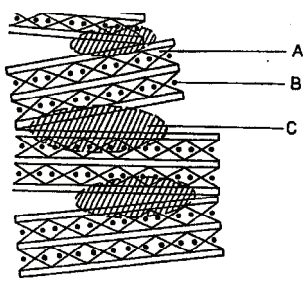

Fig.2 Schematic picture of stack assemblage in Na montmorillonite A) montmorillonite flake, B) interlamellar space, C) stack contact with interacting electrical double-layer and “disjoining” water clay (Pusch et al, 1990)

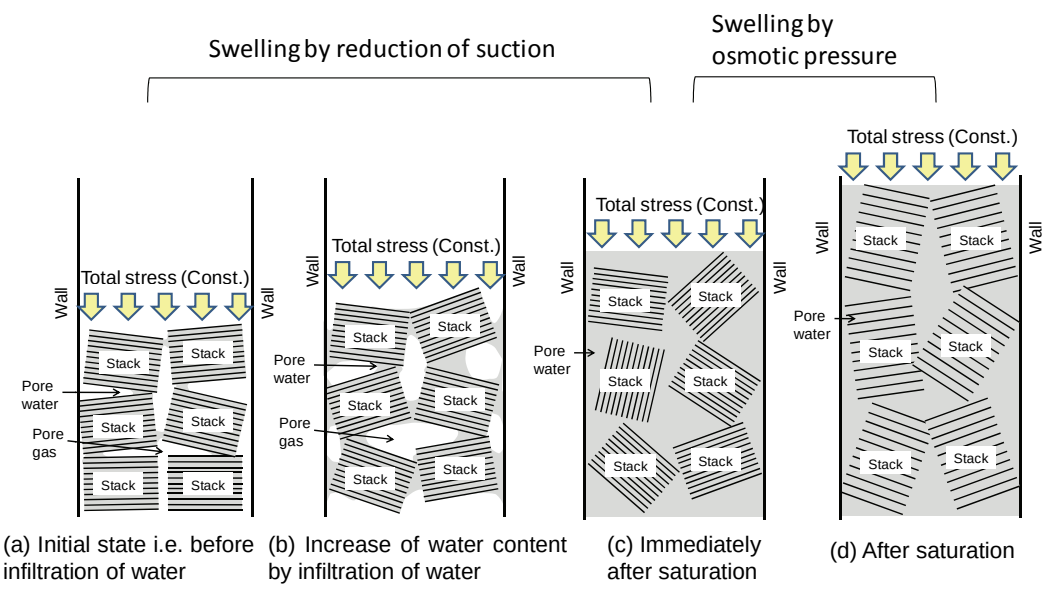

Assumed swelling mechanism of compacted bentonite during infiltration of water (This study)

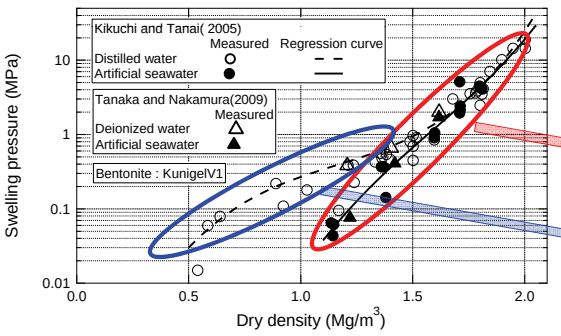

Fig.3 Results of swelling pressure test

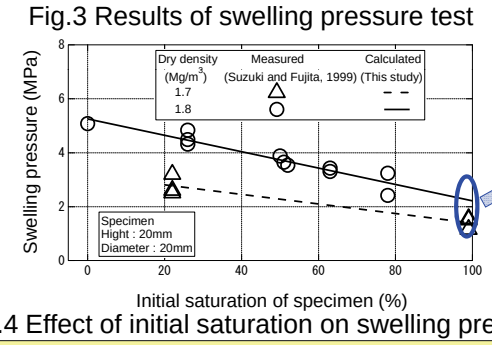

Fig.4 Effect of initial saturation on swelling pressure

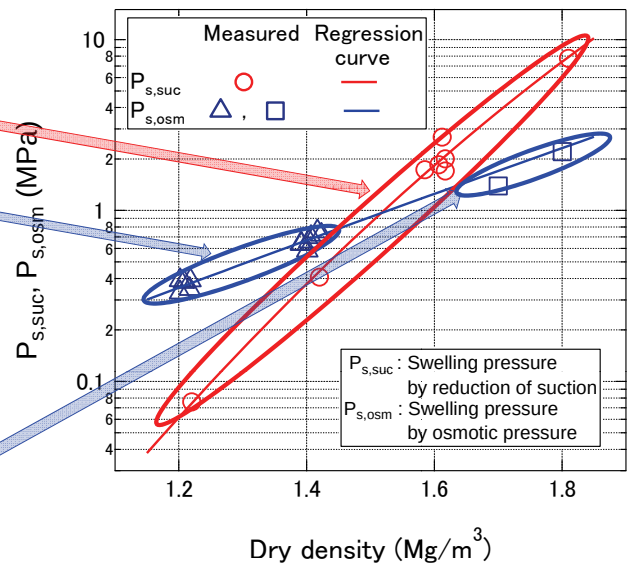

Fig.5 Relation between $P_{s,suc}$,$P_{s,osm}$ and dry density

Dry density dependency of swelling pressure of reduction of suction $P_{s,suc}$ and of osmotic pressure $P_{s,osm}$

Outline of Dual Swelling Mechanism Model proposed in this study

(a) Swelling pressure by reduction of suction, $P_{s,suc}$

$$P_{s,suc} = \int_{S_{w,e0}}^{1} \mathrm{d}\sigma'_a \cdot \mathrm{d}S_{w,e}$$

where, $S_{w,e}$, $S_{w,e0}$: effective saturation, initial effective saturation respectively

(b) Axial stress increment $\mathrm{d}\sigma'_a$ by reduction of suction during infiltration of water

$$\mathrm{d}\sigma'_a = \frac{\mathrm{d}K_{d1}/K_{d1} \cdot \sigma'_m - \beta \cdot S_{w,e} \cdot \mathrm{d}u_c}{1 + K_{d1}/K_{sys,a}}$$

where, σ'_m : mean effective stress, K_{d1} : one-dimensional bulk modulus, u_c : suction, $K_{sys,a}$: axial modulus of the test vessel, β : a parameter, which depends of dry density

(c) Observed Swelling pressure, P_s

$$P_s = \mathrm{Max}\left[P_{s,suc}, P_{s,osm}\right]$$

where, $P_{s,osm}$: swelling pressure by osmotic pressure

Comparison between measured results and calculated results by Dual Swelling Mechanism Model proposed in this study

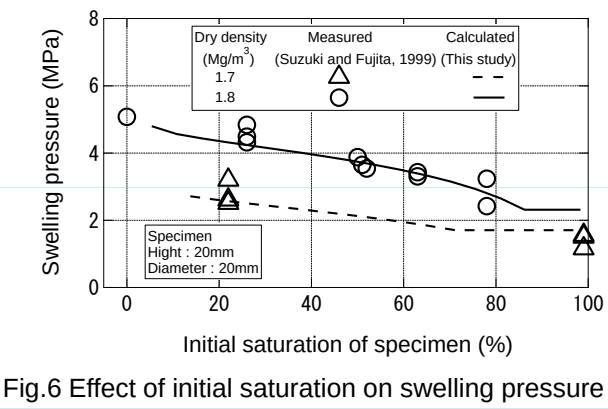

Fig.6 Effect of initial saturation on swelling pressure

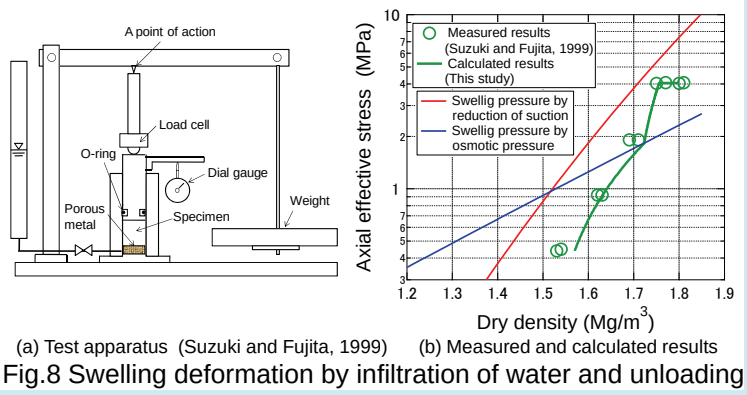

(a) Test apparatus (Suzuki and Fujita, 1999) (b) Measured and calculated results

Fig.8 Swelling deformation by infiltration of water and unloading

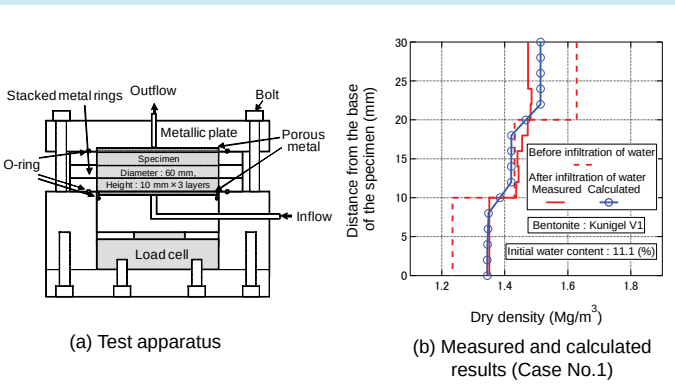

(a) Test apparatus (b) Measured and calculated results (Case No.1)

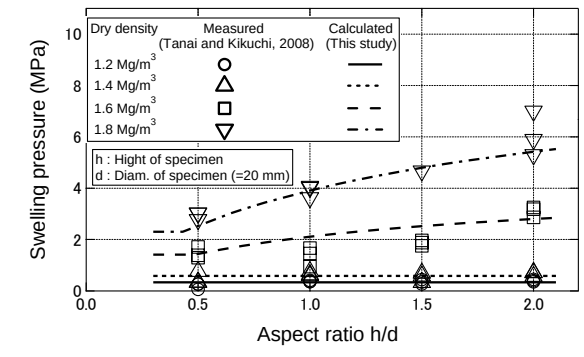

Fig.7 Scale effect of swelling pressure (Effect of aspect ratio on swelling pressure)

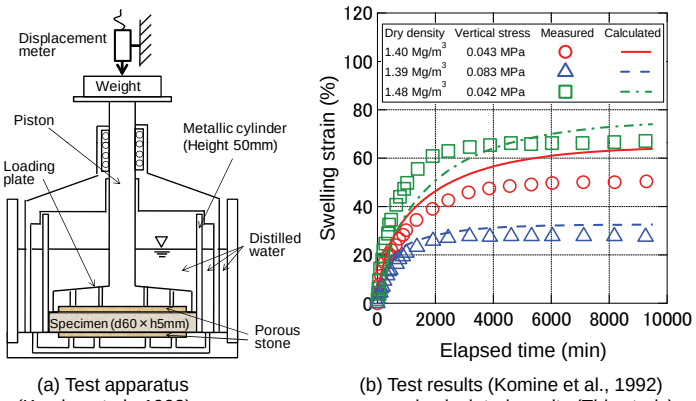

(a) Test apparatus (Komine et al., 1992) (b) Test results (Komine et al., 1992) and calculated results (This study)

Fig.9 Swelling deformation by infiltration of water

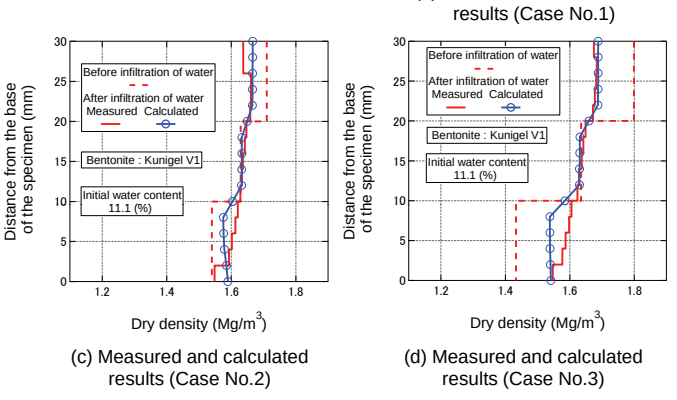

(c) Measured and calculated results (Case No.2) (d) Measured and calculated results (Case No.3)

Fig.10 Change of dry density distribution of specimens, initial dry density of which is heterogeneous, caused by infiltration of water (This study)

CONCLUSIONS

(1) Swelling of compacted bentonite is attributed not only to osmotic pressure but also to reduction of suction. Thus, a stress-strain model named dual swelling mechanism model for compacted bentonite is proposed in this paper. It is assumed in the proposed model that swelling by osmotic pressure occurs only when bentonite is fully saturated, while swelling by reduction of suction occurs only when bentonite is unsaturated.

(2) Using the proposed model, the effect of initial saturation on swelling pressure, which was already reported by Suzuki and Fujita(1999), can be simulated with accuracy. The effect of aspect ratio of the specimen on swelling pressure, which was already reported by Tanai and Kikuchi(2008), can be also simulated with accuracy by the model.

(3) Swelling deformation of the specimen caused by infiltration of water under unloading as well as under constant vertical load conditions can be simulated by the proposed model with accuracy considering axial modulus of the test vessel.

(4) Change of dry density distribution of a specimen with initially heterogeneous dry density can be simulated with accuracy.

F.3：Paper－Modeling hydraulic conductivity and swelling pressure of several kinds of bentonites affected by salinity of water (ICEM 2010-40013)

Proceedings of the ASME 13th International Conference on Environmental Remediation and Radioactive Waste Management
ICEM2010
October 3-7, 2010, Tsukuba, Japan

ICEM2010-40013

MODELING HYDRAULIC CONDUCTIVITY AND SWELLING PRESSURE OF SEVERAL KINDS OF BENTONITES AFFECTED BY SALINITY OF WATER

Yukihisa Tanaka
Central Research Institute of Electric Power Industry
Abiko-shi, Chiba-ken, Japan

Takuma Hasegawa
Central Research Institute of Electric Power Industry
Abiko-shi, Chiba-ken, Japan

Kunihiko Nakamura
Central Research Institute of Electric Power Industry
Abiko-shi, Chiba-ken, Japan

ABSTRACT

In case of construction of repository for radioactive waste near the coastal area, the effect of salinity of water on hydraulic conductivity as well as swelling pressure of bentonite as an engineered barrier should be considered because it is known that the hydraulic conductivity of bentonite increases and swelling pressure decreases with increasing salinity of water. Though the effect of salinity of water on hydraulic conductivity and swelling pressure of bentonite has been investigated experimentally, it is necessary to elucidate and to model the mechanism of the phenomenon because various kinds of bentonites may possibly be placed in various salinities of ground water. Thus, in this study, a model for evaluating hydraulic conductivity as well as swelling pressure of compacted bentonite is proposed considering the effect of salinity of water as follows :

a) Change in number of flakes of a stack of montmorillonite because of cohesion
b) Change in viscosity of water in interlayer between flakes of montmorillonite.

Quantitative evaluation method for hydraulic conductivity and swelling characteristics of several kinds of bentonites under saline water is proposed based on the model mentioned above.

Key Words **:** *radioactive waste disposal, bentonite, hydraulic conductivity, seawater, modeling*

INTRODUCTION

Though engineering properties of compacted bentonite have been investigated considerably, almost studies have been carried out under distilled water or deionized water condition. At the greater depth, however, salinity of ground water becomes higher near the coastal area. Thus, the effect of saline water should be considered in the case of construction of repository for nuclear waste near the coastal area (Fig.1). The effect of sea water on permeability as well as swelling characteristics of bentonite has been investigated experimentally by several researchers [1-3]. However, though it is necessary to elucidate and to model the mechanism of the phenomenon from a view point of quality assurance because various kinds of bentonites with distributed density may possibly be placed in various salinities of ground water, researches of modeling the effect of saline water have not been conducted sufficiently. Thus, in this study, modeling swelling characteristics and permeability of several compacted bentonites affected by salinity of water is conducted. Further validity of the model is confirmed by comparing the calculated results by the model with the results of laboratory experiments.

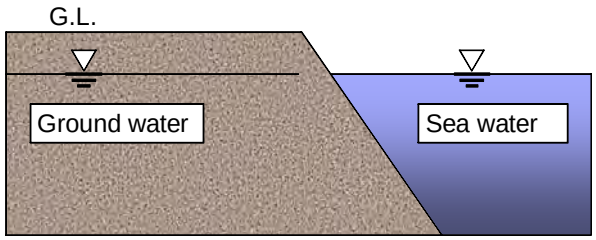

Fig.1 Conceptual distribution of saline water in coastal area

In this paper, “100% concentration” means that salinity of the artificial seawater approximates that of natural seawater, while “10% concentration” and “50% concentration” mean percentage of salinity to the “100% concentration” and are 10% and 50%, respectively.

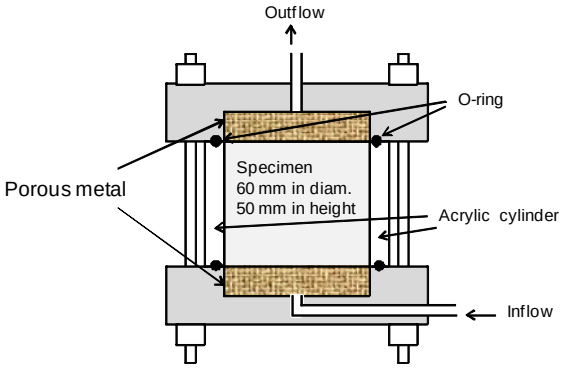

(a) Permeability test apparatus [1]

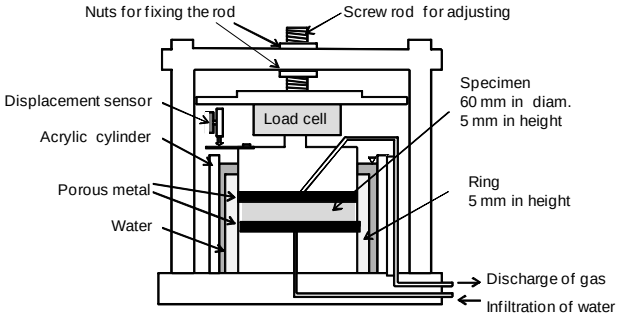

(b) Swelling pressure test apparatus [4]

Fig.2 Test apparatuses mainly used in this study

Table 1 Properties Bentonites used in this study [4]

Name	KunigelV1	Volclay	Kunibond	Neokunibond
	Sodium bentonite	Sodium bentonite	Calcium bentonite	Transformed sodium bentonite
Producing district	Tsukinuno inYamagata Pref., JAPAN	State of Wyoming, USA	Ukiyama deposit in Miyagi Pref., JAPAN	Kawasakicho in Miyagi pref., JAPAN
Density of clay particle (Mg/m^3)	2.79	2.84	2.71	2.68
Liquid limit (%)	473.9	628.2	144.5	607.5
Plastic limit (%)	26.61	44.8	63.87	50.69
Plasticity index	447.3	583.4	80.6	556.8
Activity	6.93	6.35	4.36	7.79
Plastic ratio	16.81	13.02	1.26	10.98
Clay(<2μm) content (%)	64.5	91.9	18.5	71.5
Montmorillonite content (%)	48	69	80	76
Cation exchange capacity (meq/g)	0.732	1.007	0.796	1.035
Capacity of exchangeable Na ion (meq/g)	0.405	0.566	0.119	0.62
Capacity of exchangeable Ca ion (meq/g)	0.287	0.293	0.585	0.333
Capacity of exchangeable K ion (meq/g)	0.009	0.016	0.019	0.019
Capacity of exchangeable Mg ion (meq/g)	0.03	0.132	0.072	0.063

TESTS

Methods

Permeability tests and swelling pressure tests were conducted using mainly test apparatuses shown in Fig.2 for 4 kinds of bentonites listed in Table 1. Separately from these tests, swelling pressure and permeability were measured simultaneously using the special testing apparatus illustrated in Fig.3. Diameter of the specimen for the three tests is 60 mm, while height of the specimen for the permeability test (Fig.2(a)), the swelling pressure test (Fig.2(b)) and the simultaneous measurement test (Fig.3) are 50 mm, 5 mm and 20 mm, respectively.

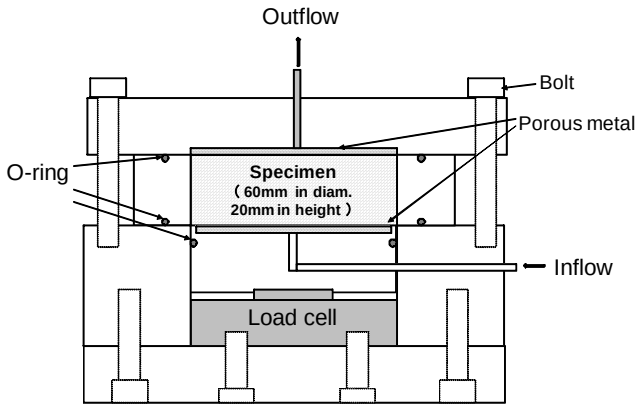

Fig.3 Test apparatus for simultaneous measurement [5]

Results

Figure 4 shows the relationships between the coefficient of permeability and dry density of bentonite. The effect of the salinity of water on permeability of sodium bentonite, such as KunigelV1 and Volclay or transformed sodium bentonite, such as Neokunibond is more considerable than that of calcium bentonite, such as Kunibond. Figure 5 shows the relationships between swelling pressure and dry density of bentonite. Swelling pressure of sodium bentonite , such as KunigelV1 and Volclay or transformed sodium bentonite, such as Neokunibond decrease as the salinity of water increases, whereas those of calcium bentonite, such as Kunibond is not affected by salinity of the water.

MODELING MICROSTRUCTURE OF MONTMORILLONITE

Effect of characteristics of montmorillonite part of bentonite on permeability of bentonite

Figure 6 shows the relationship between permeability and effective montmorillonite void ratio e_m of several kinds of compacted bentonites [1], where effective montmorillonite void ratio e_m is defined by the following equations :

$$e_m = \rho_m / \rho_{d,m} - 1 \tag{1a}$$

$$\rho_{d,m} = \rho_d \cdot R_m \Big/ \left\{ 1 - \frac{\rho_d \cdot (1 - R_m)}{\rho_{nm}} \right\} \tag{1b}$$

where, ρ_m : density of montmorillonite flake, ρ_{nm} : density

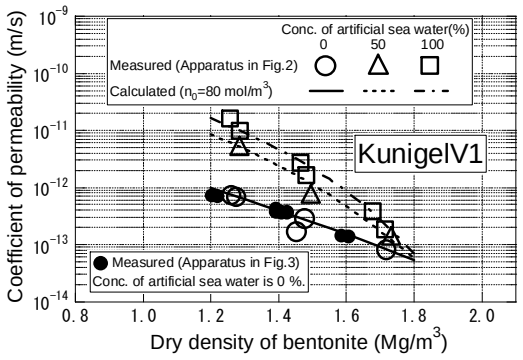

(a) KunigelV1 (Sodium bentonite)

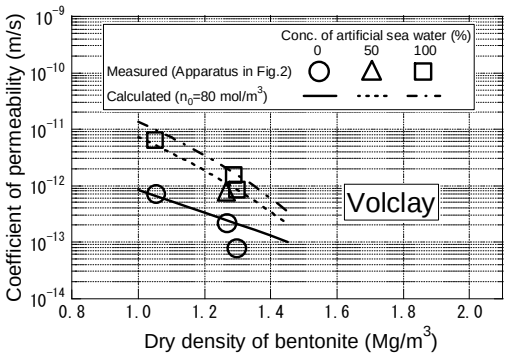

(b) Volclay (Sodium bentonite)

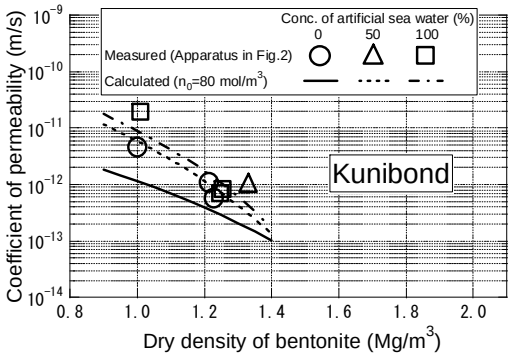

(c) Kunibond (Calsium bentonite)

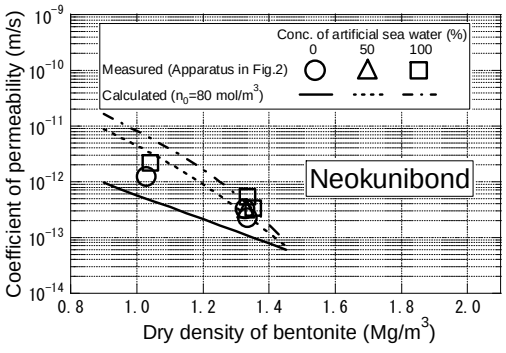

(d) Neokunibond (Transformed sodium bentonite)

Fig.4 The relationships between permeability and dry density of bentonite

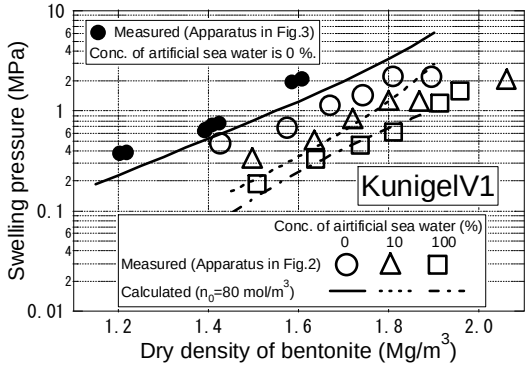

(a) KunigelV1 (Sodium bentonite)

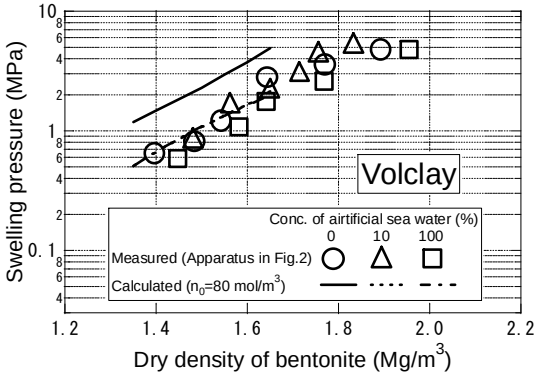

(b) Volclay (Sodium bentonite)

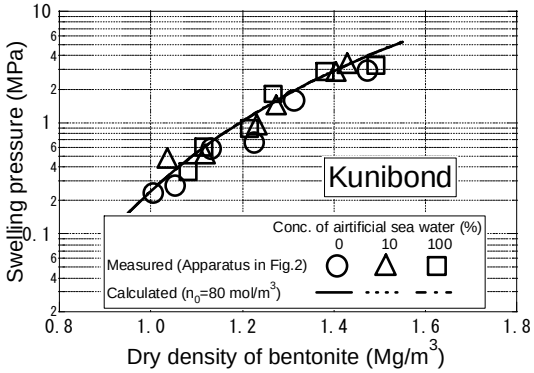

(c) Kunibond (Calsium bentonite)

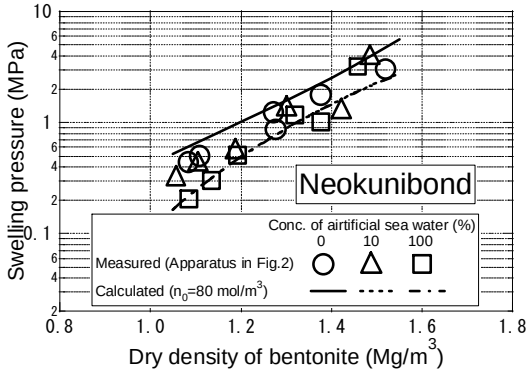

(d) Neokunibond (Transformed sodium bentonite)

Fig.5 The relationships between swelling pressure and bentonite dry density

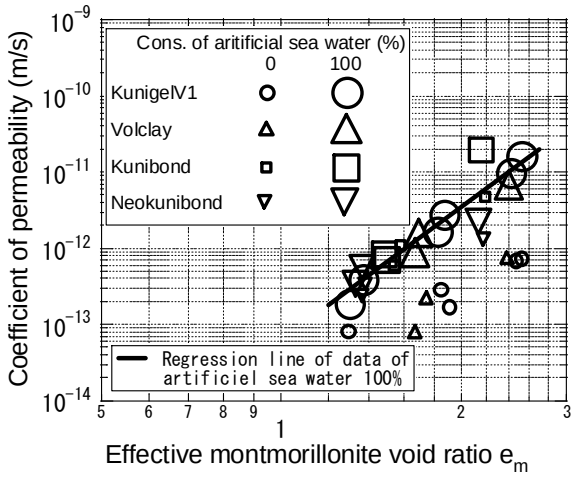

Fig.6 The relationships between coefficient of permeability and effective montmorillonite void ratio[5]

Table 2 Assumption on microstructure of montmorillonite based on summary of preceding XRD studies

Effective montmorillonite dry density ρ_{dm} (Mg/m^3)		0.32 < ρ_{dm} < 0.74	0.74 < ρ_{dm} < 1.00	1.0< ρ_{dm} < 1.3
Effective montmorillonite void ratio e_m		2.741 < e_m < 7.550	1.779 < e_m < 2.741	1.138 < e_m < 1.779
Converted bentonite dry density of bentonite KunigelV1 ρ_{db} (Mg/m^3)		0.60 < ρ_{db} < 1.20	1.20 < ρ_{db} < 1.50	1.50 < ρ_{db} < 1.80
Microstructure of flakes of mont morillonite	"0% concentration"	Straight column model	Mixture of Three water layer hydrate and two water layer hydrate	Three water layer hydrate
	"100% concentration"	Three water layer hydrate	Three water layer hydrate	Three water layer hydrate

of component minerals excluding montmorillonite, $\rho_{d,m}$: effective dry density of montmorillonite, ρ_d: dry density of bentonite, R_m : content of montmorillonite in bentonite

As shown in Fig.5, the relationship between permeability and effective montmorillonite void ratio e_m in the condition of 100% concentration, which is equivalent to that of natural seawater, of artificial seawater seems to be not affected by the kind of bentonite. Therefore it is considered that permeability of bentonite is dominated by effective montmorillonite void ratio e_m.

Effect of dry density and pore water chemistry on the microstructure of montmorillonite clay

Pucsh and Hokmark described that Na montmorillonite clay consists of 1 nm flakes forming stacks with a thickness from 50 to 200 μm depending on the bulk density and pore water chemistry [6]. Pusch and Hokmark, Pusch and Karnland also described that the interlamellar space hosts "internal", ordered water forming three hydrate at maximum [6,7], while the void separating the stacks contain water in various physical conditions ("external water"). Thus, in this paper, the water in

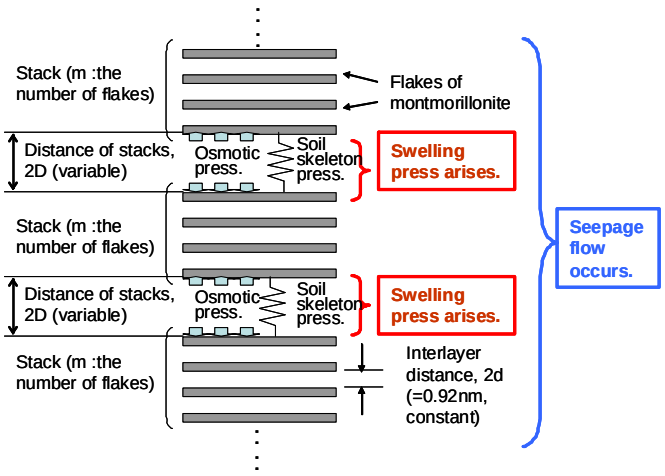

Fig.7 Assumed microstructure of montmorillonite clay

the interlamellar space and the void separating the stacks are called internal water and external water, respectively.

Several researchers conducted X-ray diffraction study on aqueous or saturated montmorillonite clay samples to investigate the microstructure of montmorillonite clay [8-10]. Table 2 was prepared for modeling microstructure of montmorillonite clay in this study by summarizing the results of these X-ray diffraction studies.

According to Table 2, the interlamellar space of montmorillonite clay with dry density ranging from 0.32 to 1.3 Mg/m^3 mostly has water forming three water layer hydrate, while microstructure of montmorillonite clay with dry density ranging from 0.32 to 0.74 Mg/m^3 is forming straight column model for distilled or deionized water. Thus, in this paper, the model shown in Fig.7 is proposed as the microstructure of montmorillonite clay. The assumptions of the model are described as follows :

1) Internal water is forming three water layer hydrates. Thus the interlayer distance, $2d$, is 0.92nm , which is constant. Thus swelling pressure by osmotic pressure is originated from the void separating the stacks.
2) The interlayer space in the stack as well as the void separating the stacks forms passageways of water.

In the microstructure of montmorillonite clay, internal montmorillonite void ratio $e_{m,d}$ and external montmorillonite void ratio $e_{m,D}$ are defined as follows :

$$e_{m,d} = \frac{(m-1)\cdot 2d_{Twlh}}{m\cdot t} \quad (2a)$$

$$e_{m,D} = \frac{2D}{m\cdot t} \quad (2b)$$

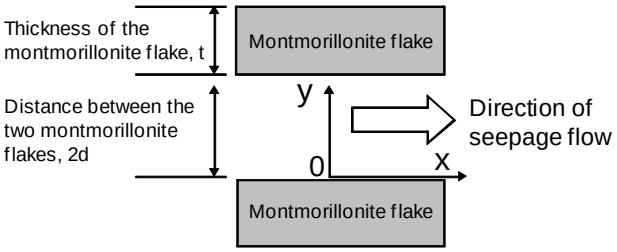

Fig.8 Coordinate systems for the seepage flow analysis

where, $2d_{Twlh}$: distance between two parallel flakes in the stack in three water hydrate state (=0.92nm), $2D$: distance between stacks, m : the number of montmorillonite flakes per one stack, t : thickness of a montmorillonite flake,

Thus there exists the following relationship among effective montmorillonite void ratio, e_m , internal montmorillonite void ratio, $e_{m,d}$, and external montmorillonite void ratio, $e_{m,D}$,

$$e_m = e_{m,d} + e_{m,D} \tag{3}$$

Though the value of m is reported to be 8 by Nakano et al.[11], the value of m is back calculated as described in the latter part of this paper.

EQUATION FOR CALCURATING PERMEABILITY OF BENTONITE

Derivation of equation for calculating mean flow velocity of internal water and external water

Figure 8 shows axes of coordinates. According to the Navier-stokes equation, one dimensional flow of water between two parallel flakes in the stack is expressed by the following equation :

$$\frac{\partial u}{\partial y} = -\frac{1}{\mu}\frac{\partial p}{\partial x}\cdot(d-y) = -\frac{\rho_w g}{\mu}\cdot i\cdot(d-y) \tag{4}$$

where, u : velocity of flow in the direction of x-axis (m/s), μ : the coefficient of viscosity of seepage water (Pa・s), ρ_w : density of seepage water (kg/m^3), p : pore water pressure in the interlamellar space (Pa), g : gravitational acceleration (=9.8 m/s^2), d : half distance between flakes in the stack

The coefficient of viscosity of water is defined as follows :

$$\tau = \mu\cdot \mathrm{d}u/\mathrm{d}y \tag{5}$$

where, τ : shear stress on the plane which is parallel to the x-axis (N/m^2)

Since fluid which consists of polar molecules such as water is absorbed by negative charge on the surface of clay particles, coefficient of permeability is decreased by the absorbing power[12]. Kato proposed the following equation considering the effect of the absorbing power on the coefficient of viscosity of water for evaluation effective diffusivity of compacted bentonite [13,14].

$$\mu = \mu_0\cdot\left\{1+\beta\cdot\left(\partial\phi(y)/\partial y\right)^2\right\} \tag{6}$$

where, μ_0 : the coefficient of viscosity of seepage water without the effect of the absorbing power (Pa・s), β : material constant (visco-elastic constant)

Substituting Eq.(6) into Eq.(4), we can obtain the following equation :

$$\frac{\partial u}{\partial y} = -\frac{1}{\mu}\cdot\frac{\partial p}{\partial x}\cdot(d-y) = \frac{\rho g}{\mu_0}\cdot i\cdot\frac{d-y}{1+\beta\cdot\left(\dfrac{\partial\phi(y)}{\partial y}\right)^2} \tag{7}$$

Integrating Eq.(7) considering $u(0)=0$, we can obtain $u(y)$ as follows :

$$u(y) = \frac{\rho g}{\mu_0}\cdot i\cdot\int_0^y \frac{d-y}{1+\beta\cdot\left(\dfrac{\partial\phi(y)}{\partial y}\right)^2}\cdot \mathrm{d}y \tag{8}$$

Consequently, the mean flow velocity of the internal water $u_{ave,d}$ is expressed as follows :

$$u_{ave,d} = \frac{\rho g\cdot i}{d\cdot\mu_0}\cdot\int_0^d\left[\int_0^y \frac{d-y}{1+\beta\cdot\left(\dfrac{\partial\phi(y)}{\partial y}\right)^2}\cdot \mathrm{d}y\right]\cdot \mathrm{d}y \tag{9}$$

In the same manner as internal water flow, the mean flow velocity of the external water flow $u_{ave,D}$ is expressed as follows :

$$u_{ave,D} = \frac{\rho g\cdot i}{D\cdot\mu_0}\cdot\int_0^D\left[\int_0^y \frac{D-y}{1+\beta\cdot\left(\dfrac{\partial\phi(y)}{\partial y}\right)^2}\cdot \mathrm{d}y\right]\cdot \mathrm{d}y \tag{10}$$

Derivation of equation for calculating coefficient of permeability

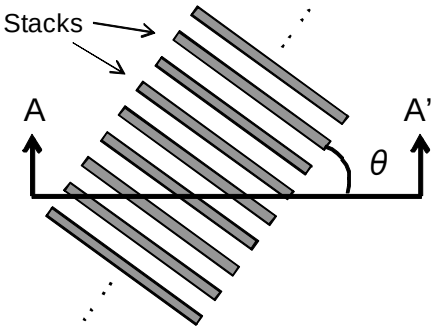

Fig.9 A-A' cross section of aligned stacks

As described previously, permeability of bentonite is dominated by the effective montmorillonite void ratio e_m. This means permeability is less affected by the montmorillonite content. Thus, in calculating coefficient of permeability, the montmorillonite content of bentonite is assumed to be 100% in this paper.

Flow rates of internal water and external water through the cylindrical specimen are expressed as follows :

$$Q_d = \frac{e_{m,d}}{1+e_m} \cdot u_{ave,d} \cdot A \tag{11a}$$

$$Q_D = \frac{e_{m,D}}{1+e_m} \cdot u_{ave,D} \cdot A \tag{11b}$$

where, A : cross section of the cylindrical specimen

Thus the apparent mean flow velocity of water, $u_{apparent}$, is expressed as follows :

$$u_{apparent} = \frac{Q_d + Q_D}{A} = \frac{e_{m,d} \cdot u_{ave,d} + e_{m,D} \cdot u_{ave,D}}{1+e_m} \tag{11c}$$

Considering randomness of the direction of seepage flow, the relationship between height of the cylindrical specimen H and the length of seepage path L is expressed as follows :

$$H = \frac{2L}{\pi} \tag{12}$$

Consequently, the relationship between the apparent hydraulic gradient of the specimen, $i_{apparent}$, and hydraulic gradient along the seepage path is expressed as follows :

$$i_{apparent} = \frac{\Delta p}{\rho g H} = \frac{\pi}{2} \cdot \frac{\Delta p}{\rho g L} = \frac{\pi}{2} \cdot i \tag{13}$$

where, Δp : pressure difference applied to the specimen in the permeability test

Consequently, according to Eqs.(11c) and (13), the coefficient of permeability of the specimen k is expressed as follows :

$$k = \frac{u_{apparent}}{i_{apparent}} = \frac{2}{\pi} \cdot \frac{e_{m,d} \cdot u_{ave,d} + e_{m,D} \cdot u_{ave,D}}{1+e_m} \cdot \frac{1}{i} \tag{14}$$

Equation for calculating swelling pressure of bentonite

Repulsive pressure of montmorillonite caused by osmotic pressure $P_{r,osm}(d)$ and attractive pressure caused by van der Waals force $P_{a,van}(d)$ are expressed as follows[5,15] :

$$P_{r,osm}(d) = 2\kappa T \cdot \left[n_1 \left\{ \cosh\left(\frac{2e'\phi(d)}{\kappa T} \right) - 1 \right\} + n_2 \left\{ \cosh\left(\frac{4e'\phi(d)}{\kappa T} \right) - 1 \right\} \right] \tag{15a}$$

$$P_{a,van}(d) = -\frac{A_h}{24\pi} \cdot \left[\frac{1}{d^3} + \frac{1}{(d+t)^3} - \frac{2}{(d+t/2)^3} \right] \cdot 10^{-6} \tag{15b}$$

where, $2d$: distance between two parallel montmorillonite flakes, A_h : the Hamaker constant (=2.2×10^{-20}J for montmorillonite) [4], n_1, n_2 : concentration of monovalence and bivalence, respectively.

n_1 and n_2 are calculated by the following equations [3] :

$$n_1 = \left(\frac{n_0}{1+e_m} \cdot r_{ben1} + n_{asw100} \cdot \frac{c_{asw}}{100} \cdot r_{asw1} \right) \cdot N_A \tag{16a}$$

$$n_2 = \left(\frac{n_0}{1+e_m} \cdot r_{ben2} + n_{asw100} \cdot \frac{c_{asw}}{100} \cdot r_{asw2} \right) \cdot N_A \tag{16b}$$

where,

n_0 : concentration of ions, which are contained in void of bentonite originally, in pore water （mol/m^3）

n_{asw100} : cation concentration of artificial seawater （=515 mol/m^3）

C_{asw} : percentage of cation concentration of diluted artificial seawater to that without dilution,

r_{ben1} : ratio of morality of monovalence cation (Na^+, K^+) to the total morality of cations contained in void of bentonite originally.

r_{ben2} : ratio of morality of bivalence cation (Ca^{2+}, Mg^{2+}) to the total morality of cations contained in void of bentonite originally (=1- r_{ben1})

r_{asw1} : ratio of morality of monovalence cation (Na^+, K^+) to the total morality of cations contained in artificial seawater.

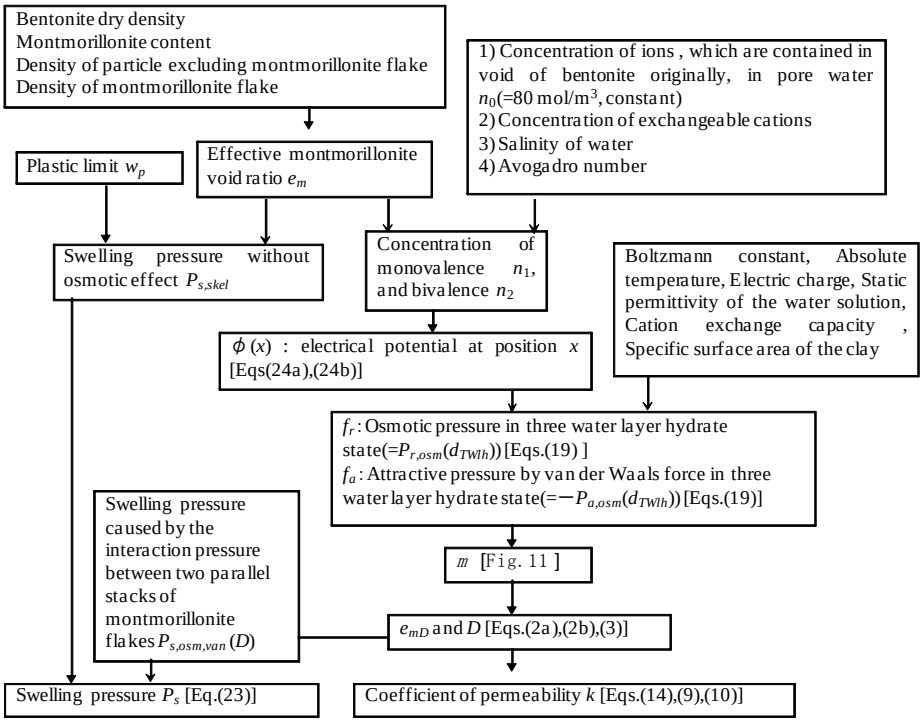

Fig.10 Procedure for calculating the coefficient of permeability and swelling pressure

r_{asw2} : ratio of morality of bivalence cation (Ca^{2+},Mg^{2+}) to the total morality of cations contained in artificial seawater. (=1-r_{asw1})

N_A : Avogadro's constant

Interaction pressure between two parallel montmorillonite flakes with distance of 2d is obtained by adding $P_{r,osm}(d)$ to $P_{a,van}(d)$.

According to the experimental results, since swelling pressure of saturated dense bentonite is isotropic [5,16], randomness in the direction of aligned stacks of montmorillonite flakes needs be considered. Normal stress applied to the A-A' cross section shown in Fig.9 is expressed as follows :

$$P_{A-A'}(d,\theta) = \cos^2\theta \cdot \left\{P_{r,osm}(d) + P_{a,van}(d)\right\} \tag{17}$$

Considering randomness of θ, swelling pressure caused by the interaction pressure between two parallel montmorillonite flakes $P_{s,osm,van}$ (d) is expressed as follows :

$$\begin{aligned} P_{s,osm,van}(d) &= \frac{2}{\pi}\cdot\int_0^{\pi/2} P_{A-A'}(d,\theta)\cdot \mathrm{d}\theta \\ &= \left\{P_{r,osm}(d) + P_{a,van}(d)\right\}\cdot\frac{2}{\pi}\cdot\int_0^{\pi/2}\cos^2\theta\cdot\mathrm{d}\theta \\ &= \frac{1}{2}\cdot\left\{P_{r,osm}(d) + P_{a,van}(d)\right\} \end{aligned} \tag{18}$$

Substituting d_{Twlh} into d of Eq.(18), swelling pressure caused by the interaction pressure between two parallel montmorillonite flakes with three water layer hydrate $P_{so,\,sm,van}$ (d_{Twlh}) can be expressed as follows :

$$P_{s,osm,van}(d_{Twlh}) = \left\{P_{r,osm}(d_{Twlh}) + P_{a,van}(d_{Twlh})\right\}/2 \tag{19}$$

Furthermore, substituting D in place d of Eq.(18), swelling pressure caused by the interaction pressure between two parallel stacks of montmorillonite flakes $P_{s,osm,van}$ (D) can be expressed as follows :

$$P_{s,osm,van}(D) = \left\{P_{r,osm}(D) + P_{a,van}(D)\right\}/2 \tag{20}$$

If swelling pressure caused by osmotic pressure is decreased considerably by the effect of saline water, swelling pressure $P_{s,skel}$ which is caused by montmorillonite clay skeleton still exists. $P_{s,skel}$ is expressed as a the function of effective montmorillonite void ratio e_m as follows [3] :

$$P_{s,skel}(e_m) = P_1 \cdot 10^{\frac{e_{m1}-e_m}{C_s}} \tag{21}$$

where, $P_{s,skel}$: swelling pressure of compacted bentonite without osmotic effect, e_m : effective montmorillonite void ratio, P_1 : reference pressure (=1 MPa), e_{m1} : e_m at P_s=P_1 without osmotic pressure, C_s : compression index of montmorillonite in one-dimensional compression (=0.915, constant),

e_{m1} can be estimated by the following equation [3] :

$$e_{m1} = 0.523 + 0.0172 \cdot w_p \tag{22}$$

where, w_p : plastic limit

If the repulsive pressure of montmorillonite caused by osmotic pressure is sufficiently large, the stacks are parallel to each other. In this case, swelling pressure observed in the swelling pressure test equals $P_{s,osm,van}(D)$ approximately. Contrary to this case, if the repulsive pressure of montmorillonite caused by osmotic pressure is small because of high salinity, the stacks will cohere and come to be not parallel to each other. In this case, swelling pressure observed in the swelling pressure test seems to equal $P_{s,skel}(e_m)$ approximately. Consequently , in this paper, swelling pressure observed in the swelling pressure test is assumed to be expressed by the following equation :

$$P_s = \mathrm{Max}\left\{P_{s,osm,van}(D)\ ,\ P_{s,skel}(e_m)\right\} \tag{23}$$

Evaluation of electrical potential distribution in internal water and external water

The equations for expressing electrical potential distribution in pore water with monovalent cation and bivalent cation using diffuse double layer theory [5]. These equations are shown as follows :

$$\frac{\mathrm{d}\phi(x)}{\mathrm{d}x} = -\sqrt{\frac{8\kappa T n_1}{\varepsilon}} \cdot \sqrt{1 + 4\frac{n_2}{n_1}\left[\cosh\frac{e'\phi(x)}{2\kappa T}\right]^2} \cdot \sinh\left\{\frac{e'\phi(x)}{2\kappa T}\right\} \tag{24a}$$

$$\frac{e'\phi(x)}{2kT} = \cosh^{-1}\left\{\sqrt{\frac{(1 + C\cdot A(x))^2 \cdot n_1}{(1 - C\cdot A(x))^2 \cdot n_1 - 16C\cdot A(x)\cdot n_2}}\right\} \tag{24b}$$

where,

$$C = \frac{Y(0)+1}{Y(0)-1} \cdot \frac{\dfrac{(n_1 + 4n_2 Y(0))}{\sqrt{n_1 + 4n_2}} + \sqrt{n_1 + 4n_2 Y(0)^2}}{\dfrac{(n_1 - 4n_2 Y(0))}{\sqrt{n_1 + 4n_2}} + \sqrt{n_1 + 4n_2 Y(0)^2}} \tag{25a}$$

$$Y(0) = \cosh\left[\sinh^{-1}\left\{\frac{1}{\sqrt{8\varepsilon n_1 \kappa T}} \cdot 96.5 \cdot \frac{CEC}{S}\right\}\right] \tag{25b}$$

$$A(x) = \mathrm{Exp}\left(\sqrt{n_1 + 4n_2}\sqrt{\frac{8e'^2}{\kappa T \varepsilon}}\, x\right) \tag{26}$$

where, x : position from the surface of the montmorillonite flake, $\phi(x)$: electrical potential at position x, κ : Boltzmann constant (=1.38×10^{-23} J/K), T : absolute temperature (K), e' : electric charge (=1.602×10^{-19} C), ε : static permittivity of the water solution (C^{2}J^{-1}m^{-1}), CEC : cation exchange capacity (meq./g), S : specific surface area of the clay (m^2/g)

COMPARIZON BETWEEN EXPERIMENTAL AND CALCULATED RESULTS

Determination of principal parameters

Figure 10 shows the procedure of calculating permeability k and swelling pressure P_s of compacted bentonite measured in the laboratory. Methodology for determining principal parameters n_0, β and m in Fig.10 are explained here.

a) The value of n_0

As the same as the previous report[3], the value of n_0 was determined to be 80 (mol/m^3) as a result of parameter fitting.

b) The value of β

The value of β is determined to be 10.2×10^{-16} (m^2/V^2), which is the value used for evaluating effect of electrical field on effective diffusivity of compacted bentonite [13,14].

c) The value of m

Since it is said that the thickness of the stack of the montmorillonite flakes varies depending on the bulk density and pore water chemistry [6], the value of m , which is defined as the number of montmorillonite flakes per stack, may vary depending on effective montmorillonite void ratio and salinity of pore water. Thus the value of m was calculated by conducting the procedure shown in Fig.10 backwards using the results of permeability test and swelling pressure test.

When cohesion occurs, the value of m increases. It is generally said that cohesion is likely to occur as the difference between attractive force and repulsive force between the clay particles [17]. Further, according to Table 2, distance between montmorillonite flakes of "100% concentration" water is 2 d_{Twlh}.

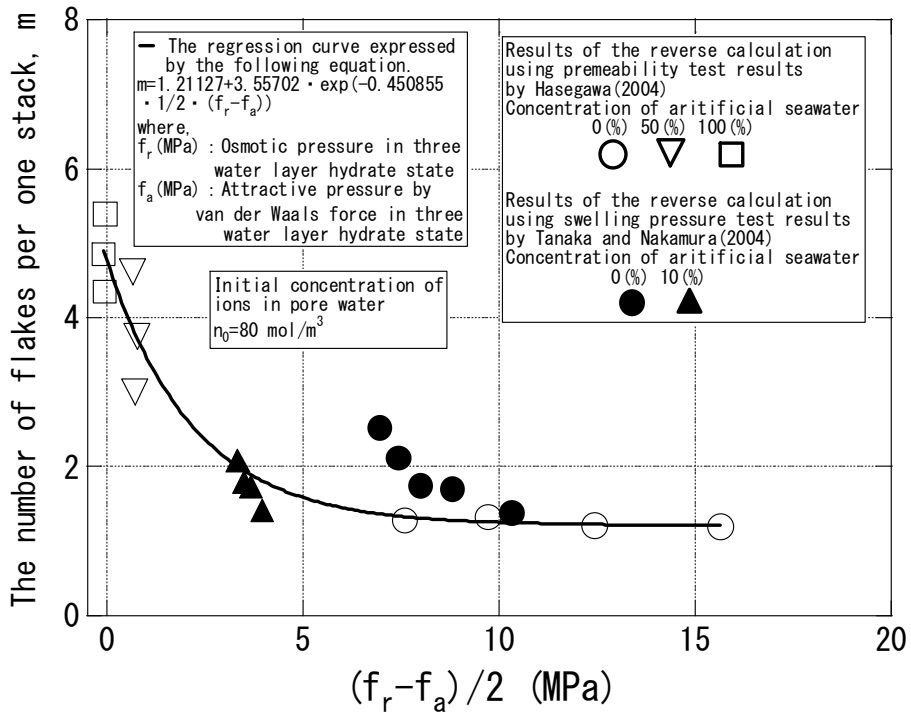

Fig.11 The inversely calculated relationship between m and $(f_r\text{-}f_a)/2$

Thus the relationships between m and $P_{s,osm,van}(d_{Twlh})$ are investigated. The relationship between m and $P_{s,osm,van}(d_{Twlh})$, which is obtained by Eq.(21), is shown in Fig.11. As the value of $P_{s,osm,van}(d_{Twlh})$ decreases, the value of m increases. This tendency seems to be attributable to the effect of cohesion because occurrence of cohesion becomes difficult with increasing in the value of $P_{s,osm,van}(d_{Twlh})$.

As shown in Fig.11, the value of $P_{s,osm,van}(d_{Twlh})$ increases, the value of m seems to approach unity, which means individual montmorillonite flakes become aligned at equal spaces as shown as the straight column model in Table 2. It seems reasonable that microstructure of montmorillonite resembles to the straight column model because of the sufficiently large value of $P_{s,osm,van}(d_{Twlh})$.

Comparison between experimental and calculated results using the back calculated m value

The coefficient of permeability and swelling pressure are calculated through the procedure shown in Fig.10, where the relationship between m and $P_{s,osm,van}(d_{Twlh})$ shown as a solid curve in Fig.11 is used. The calculated results are compared with the experimental results in Figs. 4 and 5.

As for permeability of KunigelV1, the calculated results agree well with the experimental results (Fig. 4(a)). Further for bentonite excluding KunigelV1, experimental permeability can be evaluated roughly by the procedure described previously (Figs. 4(b), 4(c) and 4(d)). In Fig. 5, swelling pressure measured by the apparatus shown in Fig.3 is shown with those by the apparatus shown in Fig. 2(b). There seems difference in measured swelling pressure depending on the two kinds of test apparatus. Thus, it can be said that, as for swelling pressure of KunigelV1, the calculated results agree with the experimental results within the experimental errors. Further for bentonite excluding KunigelV1, experimental swelling pressure can be evaluated roughly by the procedure described previously (Figs. 5(b), 5(c) and 5(d)).

CONCLUSIONS

Microstructure of montmorillonite clay is proposed in this paper based on preceding studies including XRD study by other researchers. In this model, the effect of salinity of water can be expressed by the change of the number of montmorillonite flakes per stack and by the change of distribution of electrical potential in pore water. Further the equations for expressing electrical potential distribution in pore water with monovalent cations and bivalent cations are derived using the diffuse double layer theory. In this model, it is also assumed that seepage water flows through the internal void as well as through external void. The coefficient of permeability is evaluated by integrating Navier-Stokes equation considering

that viscosity distribution in pore water, while swelling pressure is evaluated considering repulsive pressure by osmotic pressure, attractive pressure by van der Waals force and pressure by montmorillonite clay skeleton.

As for the coefficient of permeability of KunigelV1, the calculated results agree well with the experimental results. Further for bentonite excluding KunigelV1, experimental permeability can be evaluated roughly by the procedure proposed in this paper. It can be said that measured swelling pressure varies depending on the two kinds of swelling pressure test. Thus, as for swelling pressure of KunigelV1, the calculated results agree with the experimental results within the experimental errors. Further for bentonites excluding KunigelV1, experimental swelling pressure can be evaluated roughly by the procedure proposed in this paper.

REFERENCES

[1] Hasegawa,T., 2004, Investigation on the effect of seawater to hydraulic property and wetting process of bentonite, Report of Central Research Institute of Electric Power Industry, Rep. No. N04005, (in Japanese).

[2] Kikuchi,H. and Tanai,K., 2005, Basic characteristic test of buffer / backfill material under Horonobe groundwater condition (Testing Document), JNC TN8430 2004-005. (in Japanese).

[3] Tanaka ,Y. and Nakamura,K., 2005, "Effect of seawater and high-temperature history on swelling characteristics of bentonite," Journal of Japanese Society for Civil Engineers, No.806/III-73, pp.93-111. (in Japanese).

[4] Komine , H. and Ogata, N., 1999, Evaluation for swelling characteristics of buffer and backfill materials for high-level nuclear waste disposal, - Influence of sand-bentonite content and cation compositions in bentonite -, Report of Central Research Institute of Electric Power Industry, Rep. No. U99013. (in Japanese).

[5] Tanaka, Y., Hasagawa, T. and Nakamura, K., 2007, Modeling hydraulic conductivity and swelling pressure of several kinds of bentonites affected by concentration of saline water, Report of Central Research Institute of Electric Power Industry. (in Japanese).

[6] Pusch, R. and Hokmark, H. (1990) : "Basic model of water-and gas-flow through smectite clay buffers," Engineering Geology, **28**, pp.379-389.

[7] Pusch, R. and Karnland, O., 1986, Aspects of the physical state of smectite-adsorbed water. SKB Technical Report 86-25.

[8] Fukushima,Y., 1984, "X-ray diffraction study of aqueous montmorillonite emulsions," Clays and Clay Minerals, **32**(**4**), pp.320-326.

[9] Hasegawa, H., Nakaoka, K., Saito, N., Kawamura, K. and Ichikawa, Y. and Nattavut, T., 2002, "Long-term behavior of bentonite buffer based on microstructural approach (2) - Consideration of micro behavior of bentonite by X-ray diffraction under consolidation condition-," Proc of 57th annual meating of JSCE, CS10-041, pp.463 – 464. (in Japanese).

[10] Kozaki, T., Liu, J. and Sato, S., 2005, "Microstructure of compacted bentonite and its effects on diffusion behavior of radionuclides," Report of International workshop on waste management in Sapporo (Sapporo Workshop 2005), pp.49 -53.

[11] Nakano, M., Amemiya, Y., Fujii, K. and Ishida, T., 1984, "Infiltration and swelling pressure of constrained unsaturated soil ," Journal of JSIDRE, No. 112, pp.55-66. (in Japanese).

[12] Sato , K. and Murota, A., 1971, "Experimental study on the absorbed water for micro-seepage," Journal of JSCE, (**195**), pp.67-75. (in Japanese).

[13] Kato, H., Muroi, M., Yamada, N., Ishida, H. and Sato, H. , 1995, "Estimation of effective diffusivity in compacted bentonite, Proceedings of Material Research Symposium," **353**, pp.277-284.

[14] Low, P. L, 1976, "Viscosity of Interlayer water in montmorillonite, Soil Science Journal," Society of America, **40**(**4**), pp.500-504.

[15] London, F., 1937, The general theory of molecule forces, Transactions of the Faraday Society, **33**(**8**).

[16] Kudo,K., Tanaka,Y., Yokokura, T. and Kitamura, I., 2005, "Investigation of measuring swelling pressure of compacted bentonite," 40th Annual meating of JGS, pp. 2573 - 2574. (in Japanese).

[17] Sposito, G., 1984, The surface chemistry of soils, Oxford University Press.

F.4：Poster－Modeling hydraulic conductivity and swelling pressure of several kinds of bentonites affected by salinity of water

Modeling Hydraulic Conductivity and Swelling Pressure of Several Kinds of Bentonite Affected by Salinity of Water

Central Research Institute of Electric Power Industry
Yukihisa Tanaka, Takuma Hasegawa and Kunihiko Nakamura

ABSTRACT : In case of construction of repository for radioactive waste near the coastal area, the effect of salinity of water on hydraulic conductivity as well as swelling pressure of bentonite as an engineered barrier should be considered because it is known that the hydraulic conductivity of bentonite increases and swelling pressure decreases with increasing salinity of water. Though the effect of salinity of water on hydraulic conductivity and swelling pressure of bentonite has been investigated experimentally, it is necessary to elucidate and to model the mechanism of the phenomenon because various kinds of bentonites may possibly be placed in various salinities of ground water. Thus, in this study, a model for evaluating hydraulic conductivity as well as swelling pressure of compacted bentonite is proposed considering the effect of salinity of water as follows :
a) Change in number of flakes of a stack of montmorillonite because of cohesion
b) Change in viscosity of water in interlayer between flakes of montmorillonite.
Quantitative evaluation method for hydraulic conductivity and swelling characteristics of several kinds of bentonites under saline water is proposed based on the model mentioned above.
Key Words **:** *radioactive waste disposal, bentonite, hydraulic conductivity, seawater, modeling*

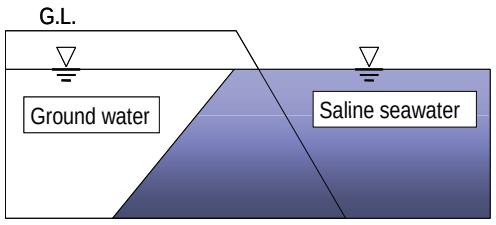

Conceptual distribution of water in coastal area

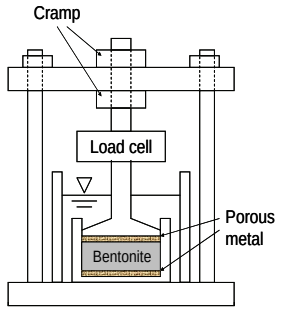

Swelling pressure test apparatus (Modified oedometer type)

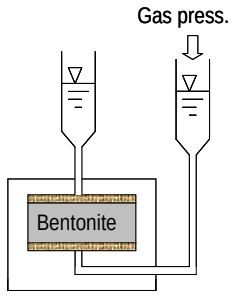

Permeability test apparatus (Box type)

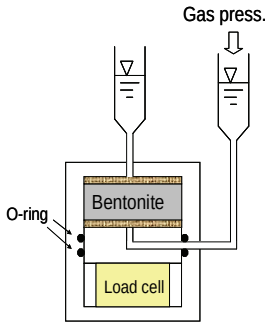

Test apparatus for simultaneous measurement (Box with load cell type)

Properties Bentonites used in this study (Komine and Ogata 1999)

Name	KunigelV1	Volclay	Kunibond	Neokunibond
	Sodium bentonite	Sodium bentonite	Calcium bentonite	Transformed sodium bentonite
Producing district	Tsukinuno inYamagata Pref., JAPAN	State of Wyoming, USA	Ukiyama deposit in Miyagi Pref., JAPAN	Kawasakicho in Miyagi pref., JAPAN
Density of clay particle (Mg/m^3)	2.79	2.84	2.71	2.68
Liquid limit (%)	473.9	628.2	144.5	607.5
Plastic limit (%)	26.61	44.8	63.87	50.69
Plasticity index	447.3	583.4	80.6	556.8
Activity	6.93	6.35	4.36	7.79
Plastic ratio	16.81	13.02	1.26	10.98
Clay(<2μm) content (%)	64.5	91.9	18.5	71.5
Montmorillonite content (%)	48	69	80	76
Cation exchange capacity (meq/g)	0.732	1.007	0.796	1.035
Capacity of exchangeable Na ion (meq/g)	0.405	0.566	0.119	0.62
Capacity of exchangeable Ca ion (meq/g)	0.287	0.293	0.585	0.333
Capacity of exchangeable K ion (meq/g)	0.009	0.016	0.019	0.019
Capacity of exchangeable Mg ion (meq/g)	0.03	0.132	0.072	0.063

Assumption on microstructure of montmorillonite based on summary of preceding XRD studies

Effective montmorillonite dry density ρ_{dm} (Mg/m^3)		$0.32 < \rho_{dm} < 0.74$	$0.74 < \rho_{dm} < 1.00$	$1.0 < \rho_{dm} < 1.3$
Effective montmorillonite void ratio e_m		$2.741 < e_m < 7.550$	$1.779 < e_m < 2.741$	$1.138 < e_m < 1.779$
Converted bentonite dry density of bentonite KunigelV1 ρ_{db} (Mg/m^3)		$0.60 < \rho_{db} < 1.20$	$1.20 < \rho_{db} < 1.50$	$1.50 < \rho_{db} < 1.80$
Microstructure of flakes of mont morillonite	"0% concentration"	Straight column model	Mixture of Three water layer hydrate and two water layer hydrate	Three water layer hydrate
	"100% concentration"	Three water layer hydrate	Three water layer hydrate	Three water layer hydrate

Equation for calculating coefficient of permeability

$$k = \frac{2}{\pi} \cdot \frac{e_{m,d} \cdot u_{ave,d} + e_{m,D} \cdot u_{ave,D}}{1 + e_m} \cdot \frac{1}{i}$$

$$u_{ave,d} = \frac{\rho g \cdot i}{d \cdot \mu_0} \cdot \int_0^d \left[\int_0^y \frac{d - y}{1 + \beta \cdot \left(\frac{\partial \phi(y)}{\partial y} \right)^2} \cdot dy \right] \cdot dy \qquad u_{ave,D} = \frac{\rho g \cdot i}{D \cdot \mu_0} \cdot \int_0^D \left[\int_0^y \frac{D - y}{1 + \beta \cdot \left(\frac{\partial \phi(y)}{\partial y} \right)^2} \cdot dy \right] \cdot dy$$

k : coefficient of permeability, φ(y) : Inner electric potential at a distance y from the surface of a montmorillonite crystal, d : half the distance between two parallel layers of crystals of montmorillonite (m), e_m : effective montmorillonite void ratio, ρ : density of pore water, g : gravitational acceleration, μ_0 : viscosity of pore water outside the diffuse double layer , β : constant, which is assumed to be 1.02×10^{-15} (m^2/V^2) by Low (1976), i : Hydraulic gradient, em.d, em,D : Internal void ratio and external void ratio, respectively.

Equations for calculating swelling pressure

$$P_s = \mathrm{Max}\left\{ P_{s,osm,van}(D) , P_{s,skel}(e_m) \right\}$$

$$P_{s,osm,van}(D) = \frac{1}{2} \cdot \left\{ P_{r,osm}(D) + P_{a,van}(D) \right\} \qquad P_{s,skel} = P_1 \cdot 10^{\frac{e_{m1} - e_m}{C_s}}$$

$$P_{r,osm}(D) = 2\kappa T \cdot \left[n_1 \left\{ \cosh\left(\frac{2e' \phi(D)}{\kappa T} \right) - 1 \right\} + n_2 \left\{ \cosh\left(\frac{4e' \phi(D)}{\kappa T} \right) - 1 \right\} \right]$$

$$P_{a,van}(D) = -\frac{A_h}{24\pi} \cdot \left[\frac{1}{d^3} + \frac{1}{(D + t)^3} - \frac{2}{(D + t/2)^3} \right] \cdot 10^{-6}$$

P_s : total swelling pressure, $P_{s,osm}$, $P_{s,skel}$: swelling pressure due to osmotic pressure and soil skeleton, respectively, $P_{a,van}$: attractive pressure by van der Waals force, φ(D) : Inner electric potential at a distance D from the surface of a montmorillonite crystal, n_1, n_2 : concentration of monovalence cation and bivalence cation, respectively, D : half the distance between two stacks, e' : charge of electron, e_m : effective montmorillonite void ratio, P_1 : reference pressure (=1 MPa), C_s : 0.847, e_{m1} : e_m at $P_{s,skel} = P_1$, the Hamaker constant , t : the thickness of a montmorillonite flake, κ : Boltzmann constant, T : absolute temperature

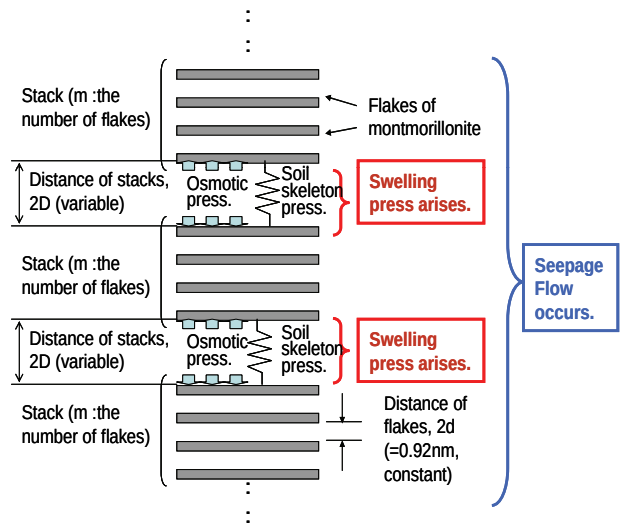

Assumed microstructure of montmorillonite clay

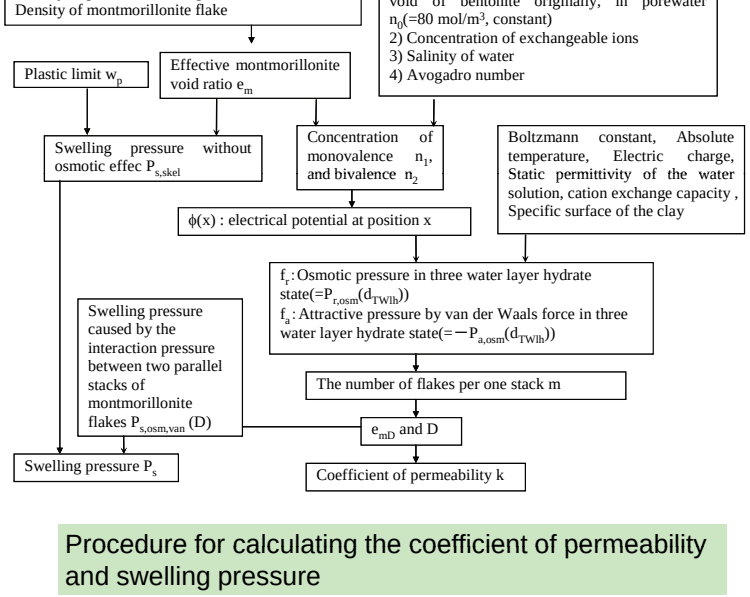

Procedure for calculating the coefficient of permeability and swelling pressure

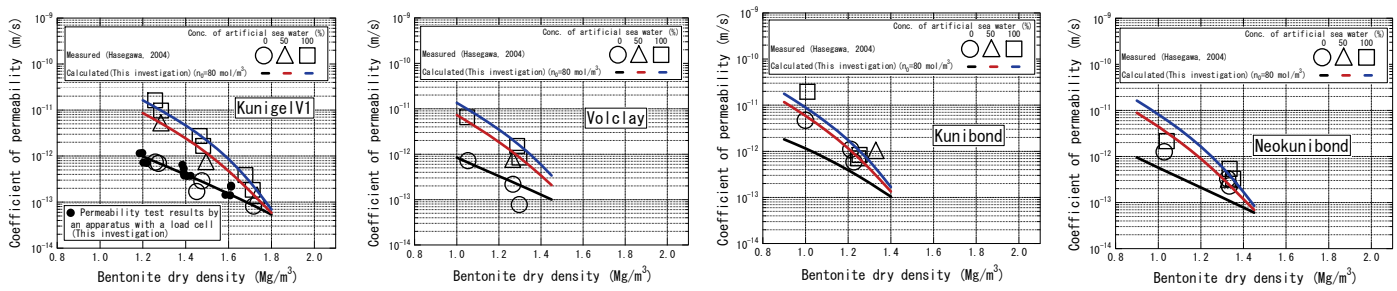

Comparison between calculated results and measured results of hydraulic conductivity

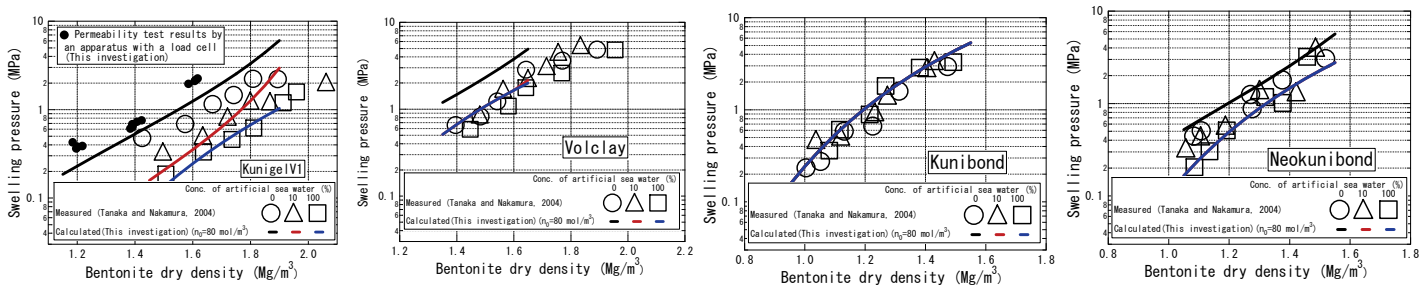

Comparison between calculated results and measured results of Swelling Pressure

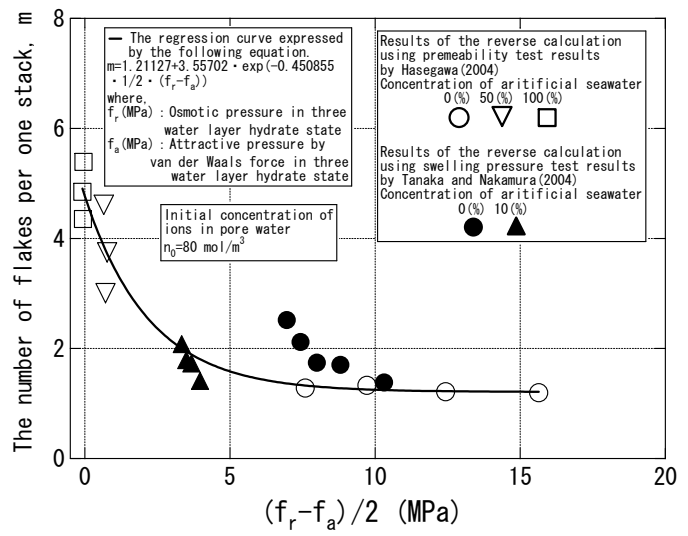

The inversely calculated relationship between m and $(f_r - f_a)/2$

CONCLUSIONS

Microstructure of montmorillonite clay is proposed in this paper based on preceding studies including XRD study by other researchers. In this model, the effect of salinity of water can be expressed by the change of the number of montmorillonite flakes per stack and by the change of distribution of electrical potential in pore water. Further the equations for expressing electrical potential distribution in pore water with monovalent cations and bivalent cations are derived using the diffuse double layer theory. In this model, it is also assumed that seepage water flows through the internal void as well as through external void. The coefficient of permeability is evaluated by integrating Navier-Stokes equation considering that viscosity distribution in pore water, while swelling pressure is evaluated considering repulsive pressure by osmotic pressure, attractive pressure by van der Waals force and pressure by montmorillonite clay skeleton.